SPECTRUM USAGE ANALYSIS AND PREDICTION USING LSTM NETWORKS

by

Anneswa Ghosh

A thesis submitted to the faculty of
The University of Utah
in partial fulfilment of the requirements for the degree of

Master of Science

in

Computer Science

School of Computing

The University of Utah

August 2020

The University of Utah Graduate School

STATEMENT OF THESIS APPROVAL

The thesis of **Anneswa Ghosh**

has been approved by the following supervisory committee members:

Sneha K Kasera	, Chair	**06/18/2020** Date Approved
Jacobus Erasmus Van Der Merwe	, Member	**06/18/2020** Date Approved
Vivek Srikumar	, Member	**06/18/2020** Date Approved

and by **Ross T Whitaker** , Chair/Dean of

the Department/College/School of **Computing**

and by David B. Kieda, Dean of The Graduate School.

ABSTRACT

The tremendous growth of wireless services has created an ever-increasing demand for the radio frequency spectrum. However, most of the spectrum, especially in the sub-6 GHz frequency ranges have been allocated. Given the observation that a large part of the allocated spectrum remains unused in various locations and at different times, dynamic spectrum access technologies that allow for opportunistic use of the allocated bands when they are idle, are being developed. In this thesis, we study the spectrum usage in the frequency range of 700 MHz to 2.8 GHz at Salt Lake City, Utah. Our study indicates that several portions of these frequencies are under-utilized, with an average of only 19% usage. Furthermore, we observe that certain frequency bands demonstrate clear usage patterns, e.g., show higher utilization during the daytime compared to night-time; that can be exploited for opportunistic secondary usage of the spectrum.

We propose a spectrum prediction system using Long Short-Term Memory (LSTM) neural networks to predict the occupancy of a channel in future time slots. We further introduce an LSTM based Window Selector to find the optimal window of future forecasts that increase the utilization of the network while minimizing the interference caused by the opportunistic user. Our experiments show that the Multivariate LSTM model can be reliably used to guide the choice of the channel for the opportunistic user. The multi-step LSTM models can be used to forecast spectrum usage with approximately 96% accuracy on the frequency bands exhibiting discernible usage patterns.

Dedicated to my sweet family, loving husband Sriram Selvam, for always being there for me and supporting me with no matter what the situation is, my mom Mrs. Rupa Ghosh and dad Mr. Anup Ghosh for working hard all their life to get me to where I am now and my little brother Dr. Kalpa Ghosh for being my best friend and always cheering me up.

TABLE OF CONTENTS

ABSTRACT iv
LIST OF TABLES viii
Chapters
1. INTRODUCTION 1
2. RELATED WORK 4
3. SPECTRUM USAGE ANALYSIS 7
3.1 Experiment Setup 7
3.2 Spectrum Power Measurement 8
3.3 Scanning Algorithm 8
3.4 Spectrum Sensing 9
3.5 Energy Detector Based Sensing 10
3.6 Analysis of the collected data 11
3.7 Broader Impact of our Spectrum Usage Study 13
4. SPECTRUM PREDICTION 28
4.1 Multi-step Univariate stacked LSTM (MSUL) 29
4.2 Single-step Multivariate stacked LSTM Network (SSML) 31
4.3 Multi-step Encoder-Decoder LSTM 32
4.4 Multi-step Multivariate Stacked LSTM (MSML) 33
5. EVALUATION 40
5.1 Evaluation Metrics 40
5.2 Baselines 41
5.3 Evaluation of Frequency Bands using SSML 42
5.4 Frequency Selection for Evaluation of Multi-step models 43
5.5 Evaluation of Multi-Step Models 44
5.6 Adaptive Threshold Mechanism 44
6. FORECAST WINDOW LENGTH 58
6.1 Forecast Window Length Selection 58
6.2 LSTM based Window Selector 59

7. DISCUSSION 64
7.1 Spectrum Usage 64
7.2 Spectrum Prediction 65
8. CONCLUSION 67

LIST OF TABLES

3.1 Range and duration of collected data 28

3.2 NUC Specifications 28

4.1 LSTM Input Dimensions 40

5.1 Selected frequencies and their usage pattern 58

6.1 Forecast window size pros and cons 64

6.2 LSTM based Window Selector RMSE 64

CHAPTER 1

INTRODUCTION

The tremendous growth of wireless services has created an ever-increasing demand for the radio frequency spectrum. However, most of the spectrum, especially in the sub-6 GHz frequency ranges have been allocated. Given the observation that a large part of the allocated spectrum remains unused in various locations and at different times, dynamic spectrum access technologies that allow for opportunistic use of the allocated bands when they are idle, are being developed. In this thesis, we study the spectrum usage in the frequency range of 700 MHz to 2.8 GHz at Salt Lake City, Utah. Our study indicates that several portions of these frequencies are under-utilized, with an average of only 19% usage. Furthermore, we observe that certain frequency bands demonstrate clear usage patterns, e.g., show higher utilization during the daytime compared to night-time; that can be exploited for opportunistic secondary usage of the spectrum.

An opportunistic secondary usage of such frequencies involves frequently scanning the bands and determining their occupancy (spectrum sensing). An opportunistic user cannot transmit in a channel before sensing and determining its occupancy, as that may cause interference. This possesses a significant challenge, as these operations need to be performed in each time slot, causing substantial delays before the user gains access leading to reduced utilization. A system that can predict the state of the channel for future

time slots can reduce the delay and the energy consumed in spectrum sensing and the decision making phase if the sensed channels are free and finalize the best channel for the opportunistic use (spectrum decision).

We propose a spectrum prediction system using Long Short-Term Memory (LSTM) neural networks to predict the occupancy of a channel in future time slots. We further introduce an LSTM based Window Selector to find the optimal window of future forecasts that increase the utilization of the network while minimizing the interference caused by the opportunistic user. Our experiments show that the Multivariate LSTM model can be reliably used to guide the choice of the channel for the opportunistic user. The multi-step LSTM models can be used to forecast spectrum usage with approximately 96% accuracy on the frequency bands exhibiting discernible usage patterns. Our contributions in this thesis are listed below:

- We build spectrum monitoring tools in the POWDER testbed and study the spectrum usage pattern for several frequency bands in Salt Lake City, Utah.
- We develop LSTM based models to forecast spectrum power values using real-world power spectral density (PSD) data that we collect.
- We also develop LSTM based architectures to forecast multiple timestep spectrum usages at once using real-world PSD data that we collect.
- We use the data collected to evaluate the performance of various deep learning models (Stacked LSTM, Encoder-Decoder LSTM, Multivariate LSTM) and compare them with the performance of two baseline approaches (Exponential Weighted Moving Average (EWMA) and Zero Rule Algorithm).

- We introduce a novel LSTM based Window Selector to select the best window to minimize interference and maximize throughput.

CHAPTER 2

RELATED WORK

The US Government is taking initiatives for allowing sharing of the under-utilized frequency bands by supporting dynamic spectrum access technologies and facilitating further research on how to effectively access the spectrum holes [1]. However, without a proper understanding of the current and future spectrum usage, these initiatives would not be able to achieve their goals. Spectrum survey is an essential tool to determine the current spectrum usage and guide the policy makers to make the most informed decision. Spectrum surveys have been conducted in San Francisco [2], Denver [3], San Diego [4]. These surveys show the maximum, minimum, and average received power levels of various bands. Spectrum survey in Singapore [5] showed that except for the bands allocated for broadcasting (analog TV, digital TV, HDTV, and DAB) services and cellular networks, most are heavily underutilized, with only 4.54% average usage in the entire frequency bands ranging from 80 MHz to 5850 MHz. In this work, we conduct a survey in Salt Lake City, Utah, to identify the frequency bands which are heavily under-utilized and the bands that exhibit predictable usage patterns.

Spectrum surveys have indicated that the frequencies are being under-utilized because of static allocation schemes [6]. This shows that several bands can be excellent candidates for spectrum sharing. Cognitive Radio Network (CRN) has been introduced to

enable unlicensed opportunistic users to communicate in idle time slots with no harmful interference to the licensed user [7]. To accomplish this, spectrum sensing must be performed. Spectrum sensing determines the current spectrum state, and to avoid any harmful interference, the opportunistic user needs to perform spectrum sensing in every time slot. Spectrum prediction can alleviate the opportunistic user from conducting spectrum sensing in every timeslot by predicting the future spectrum states. This can save a lot of time and energy, thus improving the throughput of the network [8].

A survey [9] on spectrum prediction shows that most of the existing studies are based on classical statistical techniques or shallow architecture models. While deep learning has shown promising results in many applications of image recognition, machine translation, natural language processing, target detection, etc., its use in spectrum prediction is still in its budding state [10]. Hochreiter et al. [11] introduced the Long Short Term Memory (LSTM) network to learn long-term dependencies. Predicting the state of the channel is a time-series problem that can leverage long-term dependencies learning.

The study in [12] applies deep learning to predict spectrum availability in cognitive aerospace communications; however, real-world data is converted into binary channel states like other prediction algorithms. [10] applies LSTM for spectrum prediction in the frequency hopping communication where frequency hopping sequence is also a binary time series artificially generated data. Spectrum prediction of one timestep on the power spectral density (PSD) values using LSTM is studied in [14], but one-time step prediction is not very useful for the opportunistic user. As one-time step prediction does not provide any information on the future time slots, opportunistic users need to repeatedly perform spectrum sensing in every alternate time slots. We evaluate different complex networks

with many LSTM layers to forecast power and binary occupancy states of multiple timesteps using real-world PSD values. We present extensive experimental results with real-world spectrum PSD data evaluated on Stacked LSTM network, Encoder-Decoder LSTM, and Multivariate LSTM networks. Our work differs from the existing work in the following significant ways:

1. We perform a spectrum usage study using the POWDER platform in Salt Lake City, Utah, and analyze spectrum usage patterns.
2. We develop models for multiple timestep spectrum usage forecasts using real-world power spectral density (PSD) data that we collect.
3. We evaluate the performance of various deep learning models (Stacked LSTM, Encoder-Decoder LSTM, Multivariate LSTM) and compare that with the performance of two baseline approaches (Exponential Weighted Moving Average (EWMA) and Zero Rule Algorithm).
4. We study the effects of the forecast window size and introduce a novel LSTM based Window Selector to select the best window to minimize interference and maximize throughput.

CHAPTER 3

SPECTRUM USAGE ANALYSIS

As a part of this thesis, we study the spectrum occupancy in Salt Lake City, Utah, using the resources provided by the POWDER platform. POWDER [15] is a city-scale laboratory with radio equipment, fiber infrastructure, edge-compute, and datacenter/cloud resources for research on future wireless networks.

Table 3.1 shows the frequency bands and the duration over which we collect our data. In the following sections, we discuss all aspects of our data collection in detail.

3.1 Experiment Setup

Our data is obtained using the Receive-only Fixed Endpoint installation of the POWDER Platform located at the University of Utah's main campus. The Fixed Endpoint experiment setup consists of an ensemble of Software Defined Radio (SDR) equipment from National Instruments (NI), and a compute node.

The Fixed-Endpoint equipment used for this study is NI USRP B210 SDR with its ports connected to dedicated Taoglas GSA.8841 wideband I-bar antenna. This antenna has a frequency range of 698-6000 MHz and has an approximately -2 dBi average gain across the range. The USRP is also connected to an Intel NUC, a small form factor PC, via USB 3.0. Specifications of the Intel NUC are shown in Table 3.2.

3.2 Spectrum Power Measurement

The USRP SDR device is accessed using the Python APIs provided by the USRP Hardware Driver (UHD). These APIs are used to set receive gain and to acquire I/Q samples from a specific channel at the requested sample rate.

The frequency range is divided into bands, each having a frequency width of 30MHz. Each 30MHz band is further divided into 200 points, i.e., the distance between two consecutive frequency points is 150KHz. These frequency points are represented by the center frequency of the 150KHz wide channel. The raw data collected for each frequency point is the signal power computed at the USRP.

Figure 3.2 illustrates an example of how frequency division is performed for the spectrum measurement. The example frequency range 2300-2390 MHz is divided into three sections, each of which spans 30 MHz. This 30 MHz band is further sub-divided into 200, 150 KHz channels, and the respective center frequencies are used to represent them. The upper boundary of each 150 KHz channel is shown in the top blocks of Figure 3.2.

3.3 Scanning Algorithm

The scanning algorithm carries out the measurement of frequencies, F1, F2, …, Fn in a round-robin fashion. Each Fi, where $i \in \{1, 2, \ldots, N\}$ is of width 30MHz. This process is repeated for a specified amount of time-interval, I. The scanning process is illustrated in Figure 3.3.

The details of the algorithm are shown in Figure 3.4. The frequency_list corresponds to the list of frequencies, F1, F2, …, Fn. The upper and lower frequency bound is input

into the function, which in turn is divided into 30MHz frequency bands. The function, scanning_frequencies () is executed in a while loop until the configured timer expires. The scanning_frequencies () function is responsible for acquiring raw I/Q samples at a sample rate of 30MHz through the UHD library and then processes the samples to compute log power for 150KHz bins. The time when the measurement is taken, the center frequency of 150KHz bin and log power is saved into a serialized pickle file.

A sample data collected from scanning_frequencies ([2300, 2330, …, 2360]) MHz for time_interval = 5 seconds is shown in Figure 3.5.

3.4 Spectrum Sensing

An opportunistic user needs to be aware of and sensitive to the changes in its environment. Spectrum sensing is a process of periodically monitoring frequencies aiming to identify the presence of signals and, in turn, find unused frequency bands called spectrum holes. Spectrum sensing enables opportunistic users to adapt to their surroundings by detecting spectrum holes for transmission and backing-off without causing interference when the primary user is detected.

The spectrum sensing technique which we use is based on the detection of the signal from a transmitter through local observations. As we do not have any prior knowledge about the incoming signal, we use Energy Detector based Sensing for identifying the presence of signal transmission [16].

3.5 Energy Detector Based Sensing

Energy Detector based approach does not need any prior knowledge of the signal. The signal is detected by comparing the output of the energy detector to a predefined threshold, T [19]. The decision metric of the energy detector can be written as follows:

$$S = \sum_{n=1}^{N} |y(n)|^2 \quad (1)$$

where N is the observation interval.

The decision on the occupancy of the band is made as follows:

$$D = \begin{cases} 0 & S < T \\ 1 & S \geq T \end{cases} \quad (2)$$

The threshold, T, is determined as a function of the Johnson-Nyquist thermal noise power (NP) [17,18], and the noise figure (NF).

$$T = f(NP, NF) \quad (3)$$

where,

$$NP = 10log_{10}(k\tau\Delta f \times 1000)$$

This is commonly approximated by the following equation (4) for room temperature (τ = 300 K).

$$NP = -174 + 10log_{10}(\Delta f) \quad (4)$$

where k is the Boltzmann constant, τ is the temperature, and Δf is the noise bandwidth given in Hz.

The Noise Factor (nf) of the system is defined as:

$$nf = \frac{SNR_i}{SNR_o} \quad (5)$$

SNR_i and SNR_o are the input and output signal-to-noise ratios (SNR), respectively. The noise figure (NF) is defined as the nf in decibels (dB) scale. Therefore, it is defined as follows:

$$\text{NF} = 10log_{10}(\text{nf})$$

$$= 10log_{10}(\frac{SNR_i}{SNR_o})$$

$$= 10log_{10}(SNR_i) - 10log_{10}(SNR_o)$$

$$= SNR_{i,dB} - SNR_{o,dB} \quad (6)$$

Here, $SNR_{i,dB}$ and $SNR_{o,dB}$ are the SNR values in the dB scale.
The noise figures (NF) are obtained through calibrated measurements of the RF Hardware [13].

The noise power (NP) is the electronic noise generated by the thermal agitation of the electrons inside an electrical conductor at equilibrium. This noise is present in every electrical circuit. The noise figure represents the degradation in the signal to noise ratio as the signal passes through a device in the dB scale. Hence, these two quantities help determine the minimum power needed for a signal to be detected.

3.6 Analysis of the collected data

We collected spectrum data for five days from March 8th, 2020, 11:00 PM to March 13th, 2020, 11:00 PM. The spectrogram of the frequency ranges of 700-850 MHz, 1700-1850 MHz, and 2250-2400 MHz are shown in the Figures 3.6-3.8. The x-axis represents

the time, and the y-axis represents the frequency in the spectrum occupancy plots. For better clarity of the usage pattern, we have presented the data as 300 frequencies per figure. (Example: 700 MHz to 1000 MHz, 1000 MHz to 1300 MHz, etc.). In Figures 3.9 to 3.15, the red dot indicates that the channel is occupied.

The spectrum usage in the frequency range of 700 MHz to 2800 MHz is shown in Figures 3.9 to 3.15. These figures contain the usage data for a period of 5 days along with the spectrum allocation categories by the US Department of Commerce. From these figures, it becomes evident that a vast range of frequencies is either under-utilized or not used at all. This behaviour is further illustrated in Figure 3.16, where we show the allocation categories, the frequency range, and their usage percentage.

In addition to the above observation, Figures 3.9 to 3.15 show that the usage is significantly low at night times in various frequencies. This phenomenon is illustrated in Figure 3.17. From Figure 3.17, it can be observed that there are 12 frequency ranges that show significant usage difference between day and night times. We consider 11:00 PM to 7:00 AM as our night hours.

Our major observations from the spectrum usage analysis are listed below:

1. Low or no occupancy is observed in bands allocated to Radio Navigation, Aeronautical Radio Navigation, Earth Exploration, Space Research, Amateur, and Fixed Satellite Services.
2. The average usage of the whole spectrum [700-2800 MHz] is only 19.08%.
3. The majority (71.4%) of the bands have 0-20% usage, while only 5.7% of the bands have 80-100% usage, as shown in Figure 3.18.

4. Relatively high occupancy has been observed in bands allocated for broadcasting services.
5. Among the bands that have significantly lower night-time usage, Fixed and Mobile are the common services.

3.7 Broader Impact of our Spectrum Usage Study

Spectrum usage analysis serves as a key technique in understanding the usage of the spectrum at a location and also serves as an important step towards research on dynamic spectrum access and cognitive radio technologies. This process involves interacting with the UHD library to collect raw IQ, computing power from the IQ samples, and finding an appropriate threshold to determine the occupancy for first-time users.

For ease of future POWDER platform users, we will make the code for spectrum analysis, an open-source project in GitHub. This software can either serve as a tool for researchers to gain an overall idea of current spectrum usage or as a building block for projects that require spectrum data collection. The primary contributions of our tool are as follows:

1. Support to interact with USRP using UHD libraries
2. Support to select multiple frequency ranges for scanning
3. Allows users to selectively apply threshold value on collected data
4. Support to schedule data collection for different durations ranging from minutes to weeks
5. PyPlot based advanced spectrogram analysis for data exploration without threshold

6. Robust PyPlot based visual analysis of spectrum usage
7. Supports grouping frequencies and providing comprehensive usage report

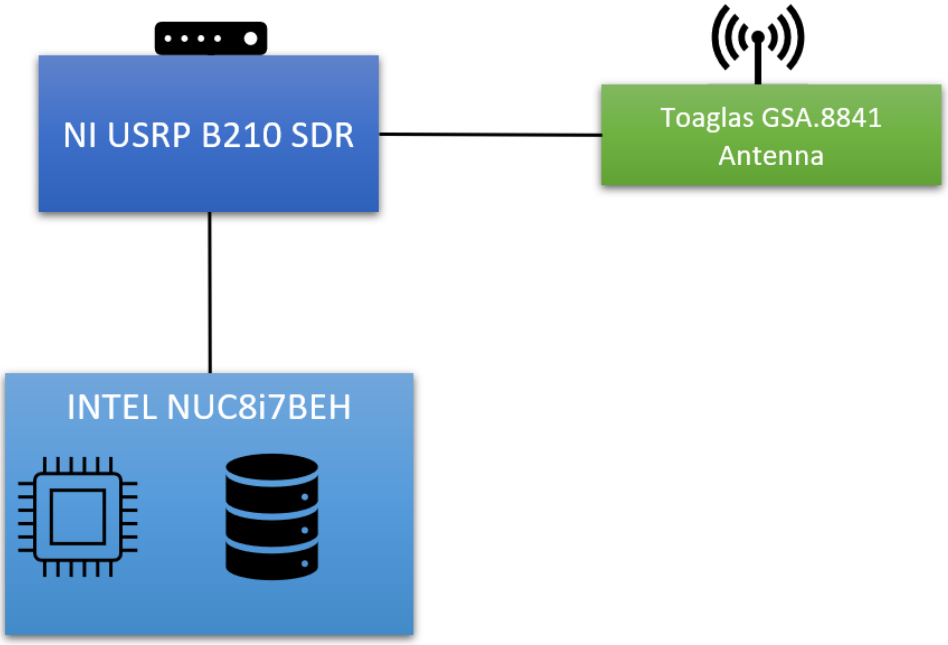

Figure 3.1 Experiment Setup

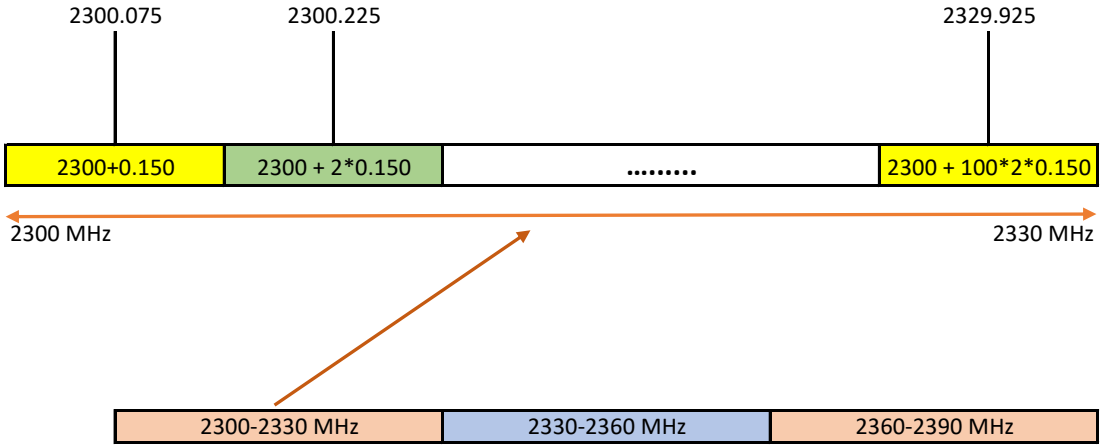

Figure 3.2 Illustration of frequency division in data collection

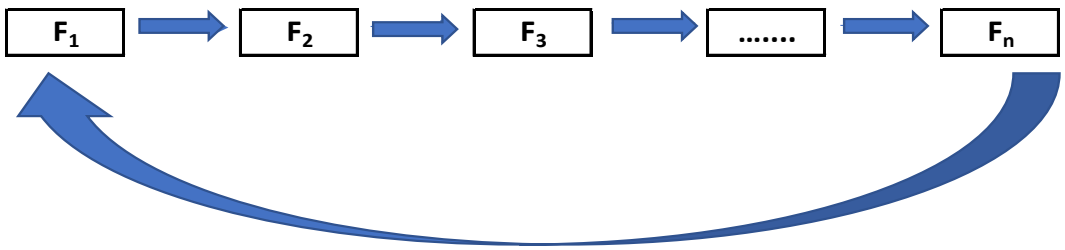

Figure 3.3 Scanning of frequencies

```
scanning_frequencies (frequency_list):
{
    For freq in the frequency_list:
        Samples = Acquire I/Q samples using UHD library
        Samples = FFT (Samples)
        Number_of_bins = 30MHz/150KHz
        For idx in Number_of_bins:
            bin_center = center frequency of the 150KHz bin
             Power = compute power of the samples of width 150KHz
             Convert power to log power.
             Save time, bin_center, log-power using pickling
}
Signal_measurement_invoker (time_interval, frequency_list):
 {
    start_time = current_time
    While (current_time – start_time <= time_interval):
        Execute Scanning_frequencies (frequency_list)
}
```

Figure 3.4 Scanning Algorithm

```
[[datetime.datetime(2020, 4, 29, 0, 46, 52)  2300.075  -93.19098757583771]
[datetime.datetime(2020, 4, 29, 0, 46, 52)  2300.375  -92.74573399088824]
…….
[datetime.datetime(2020, 4, 29, 0, 46, 57)  2359.925  -93.19892537199718]]
```

Figure 3.5 Sample data collected from scanning frequencies

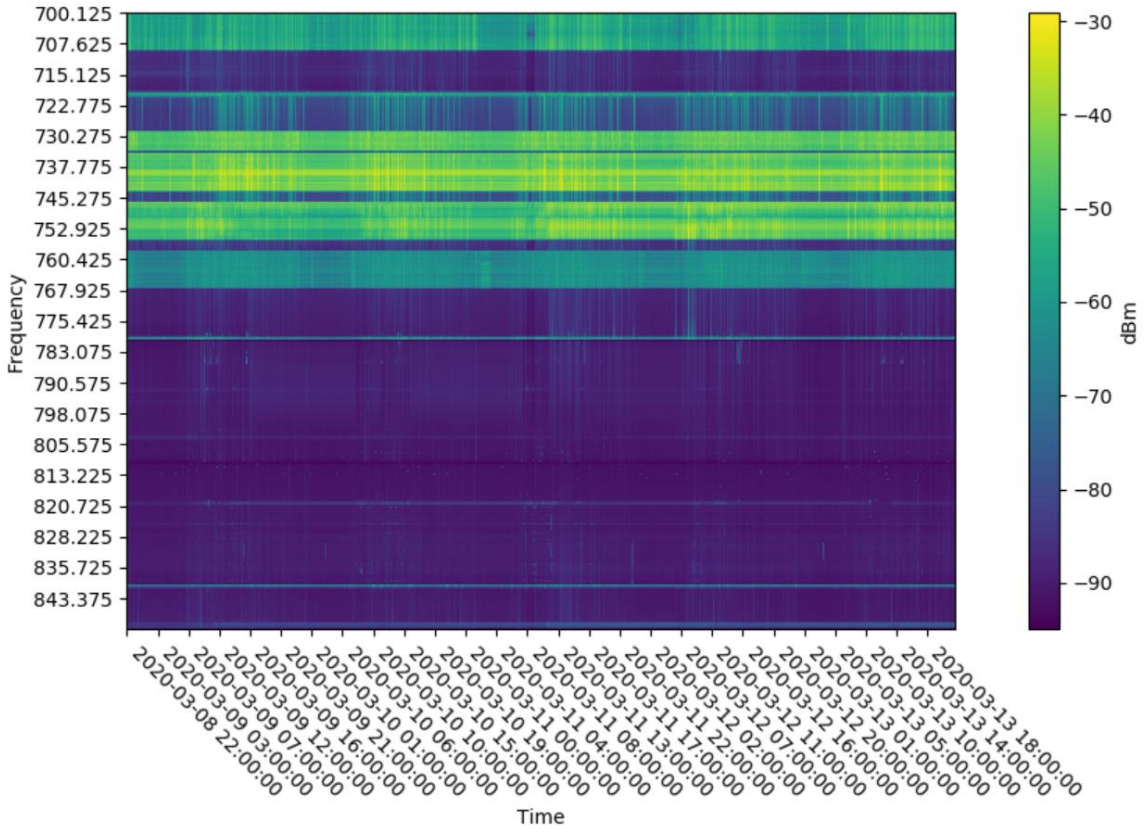

Figure 3.6 Spectrogram of 700-850 MHz

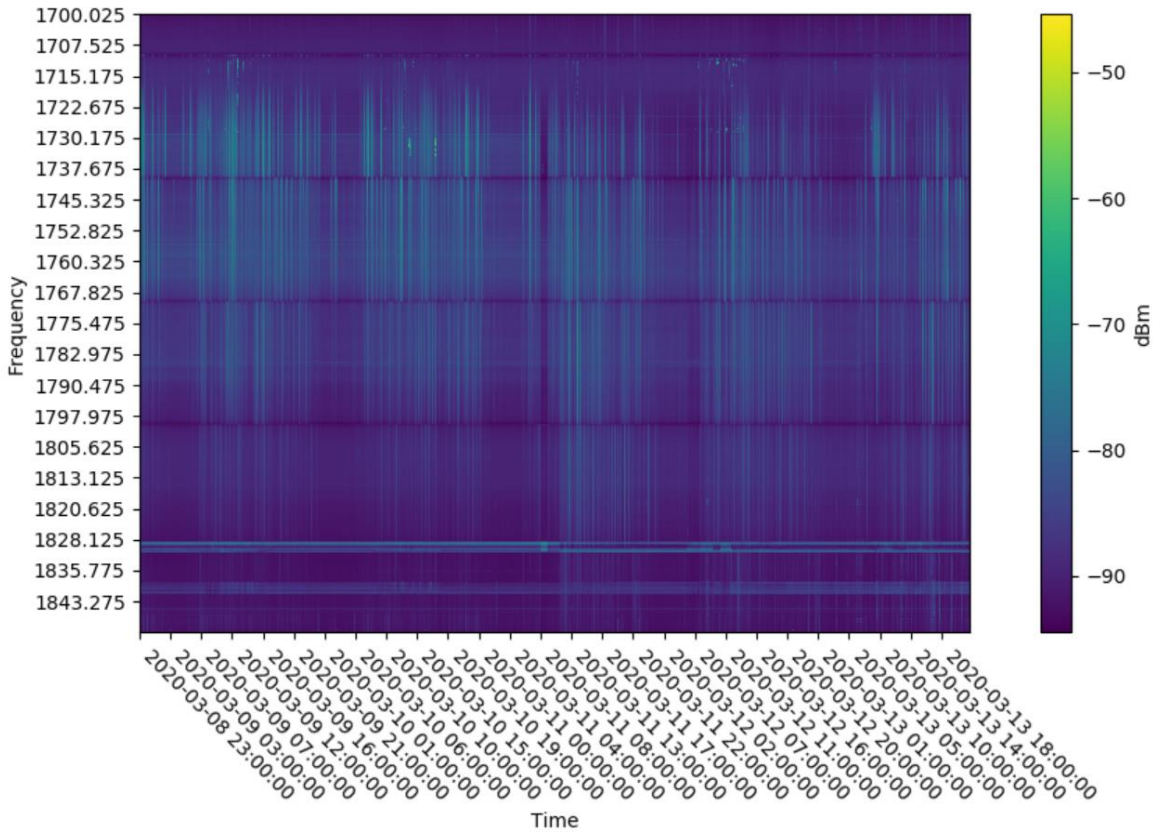

Figure 3.7 Spectrogram of 1700-1850 MHz

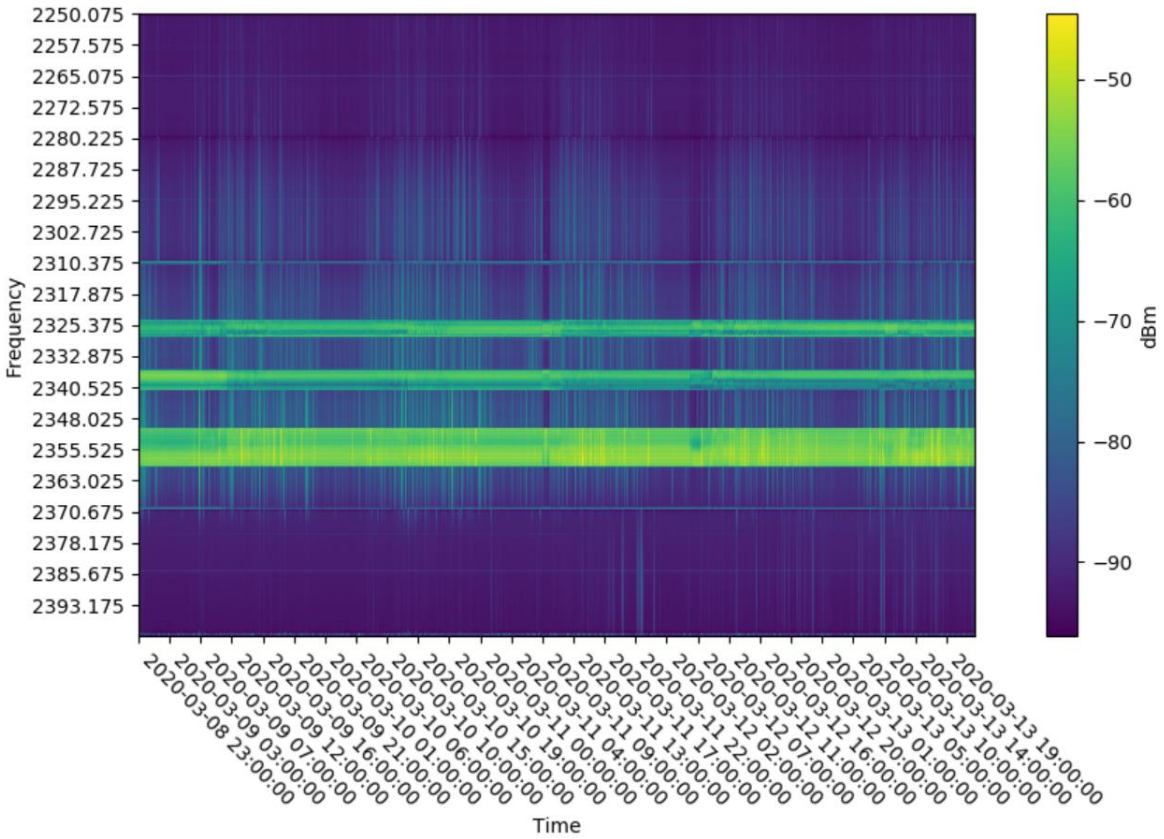

Figure 3.8 Spectrogram of 2250-2400 MHz

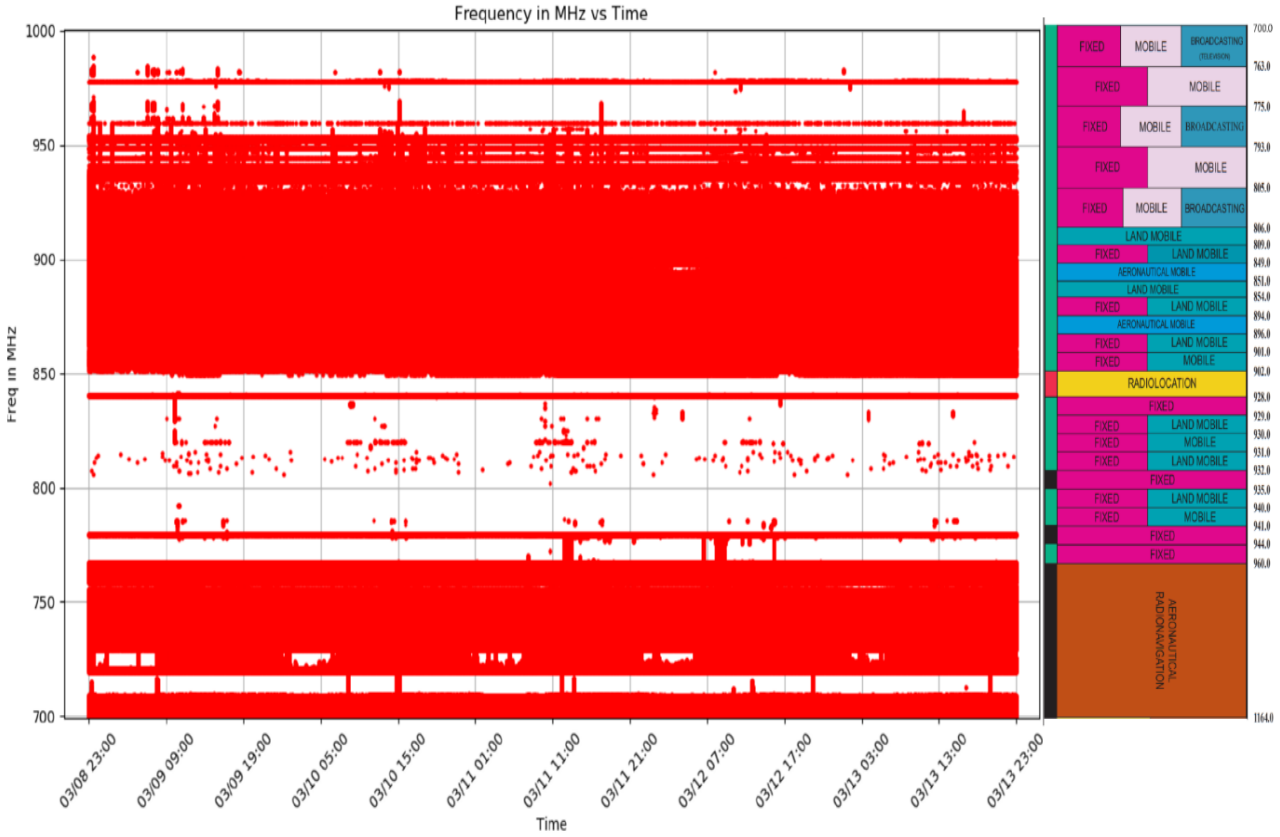

Figure 3.9 700 MHz to 1000 MHz Spectrum Allocation and Usage

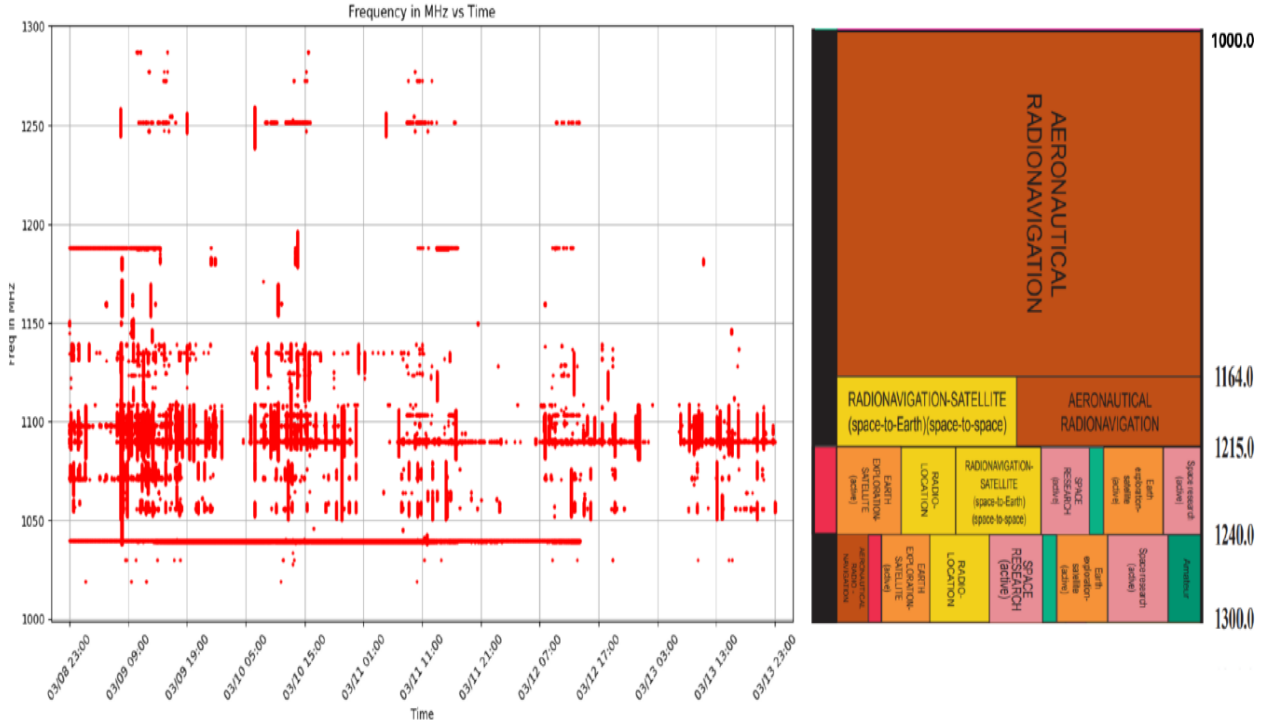

Figure 3.10 1000 MHz to 1300 MHz Spectrum Allocation and Usage

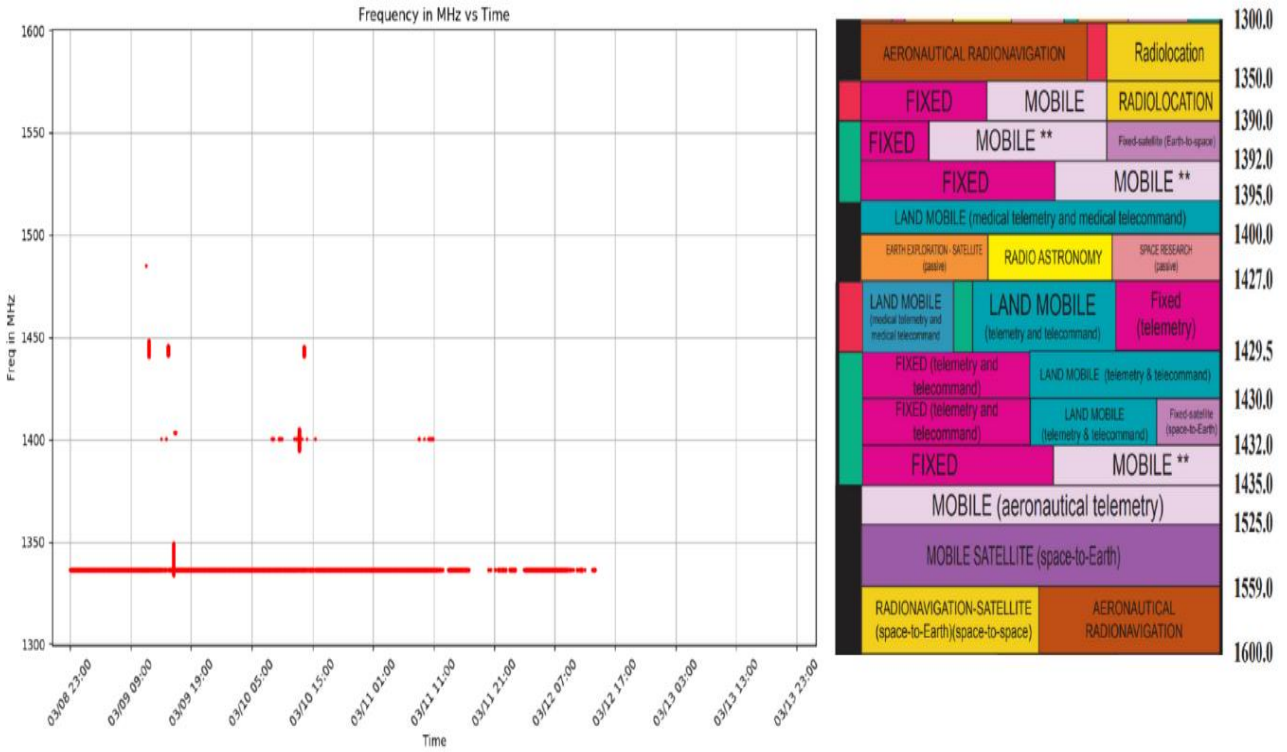

Figure 3.11 1300 MHz to 1600 MHz Spectrum Allocation and Usage

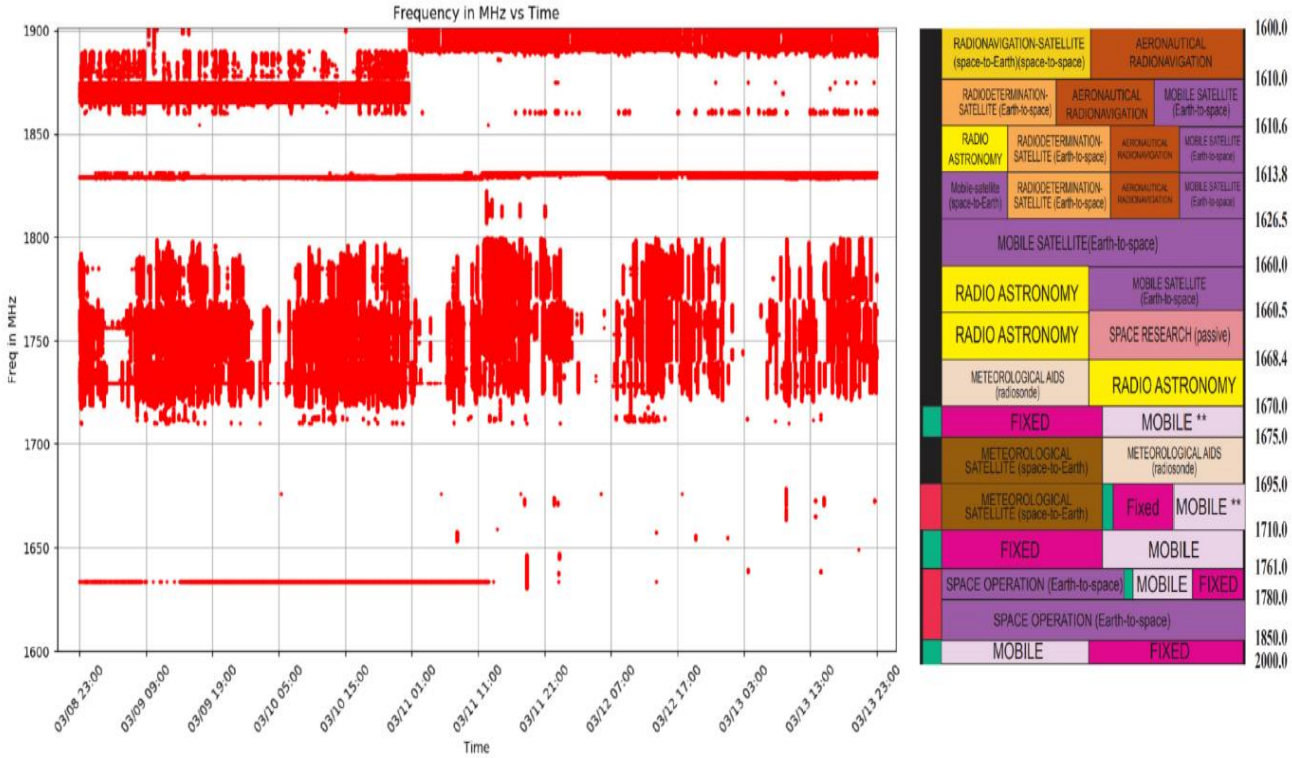

Figure 3.12 1600 MHz to 1900 MHz Spectrum Allocation and Usage

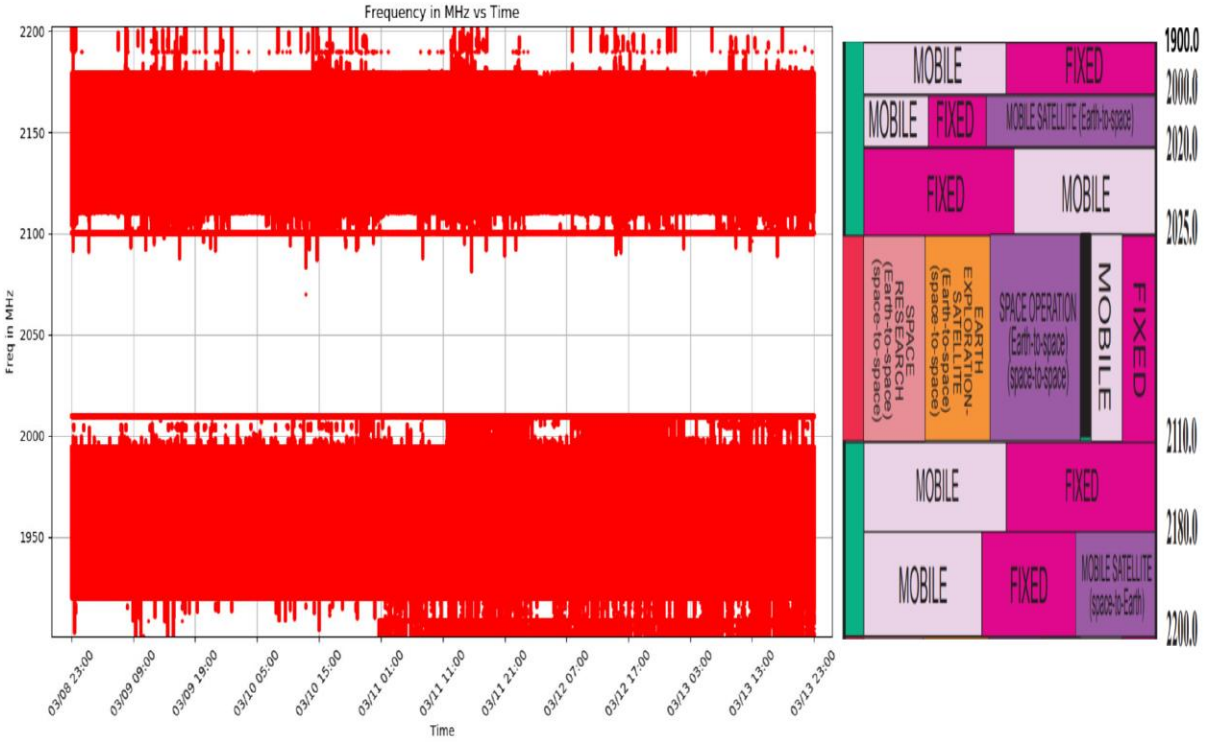

Figure 3.13 1900 MHz to 2200 MHz Spectrum Allocation and Usage

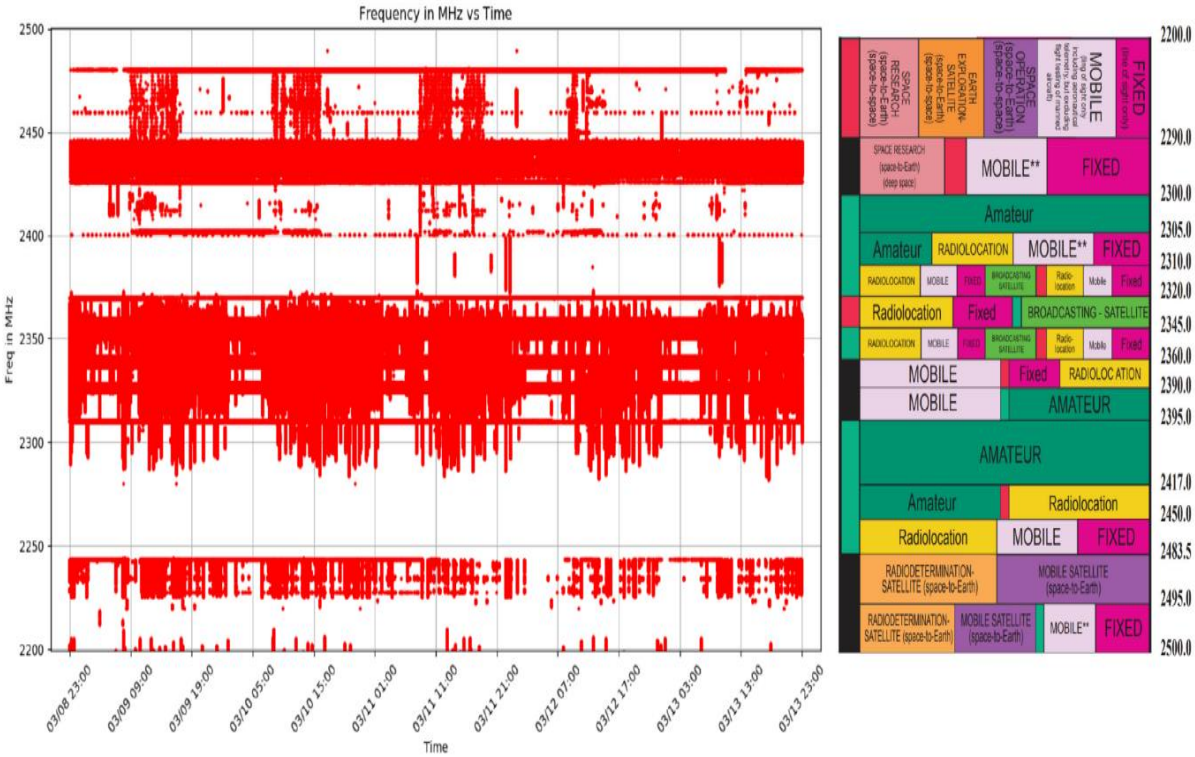

Figure 3.14 2200 MHz to 2500 MHz Spectrum Allocation and Usage

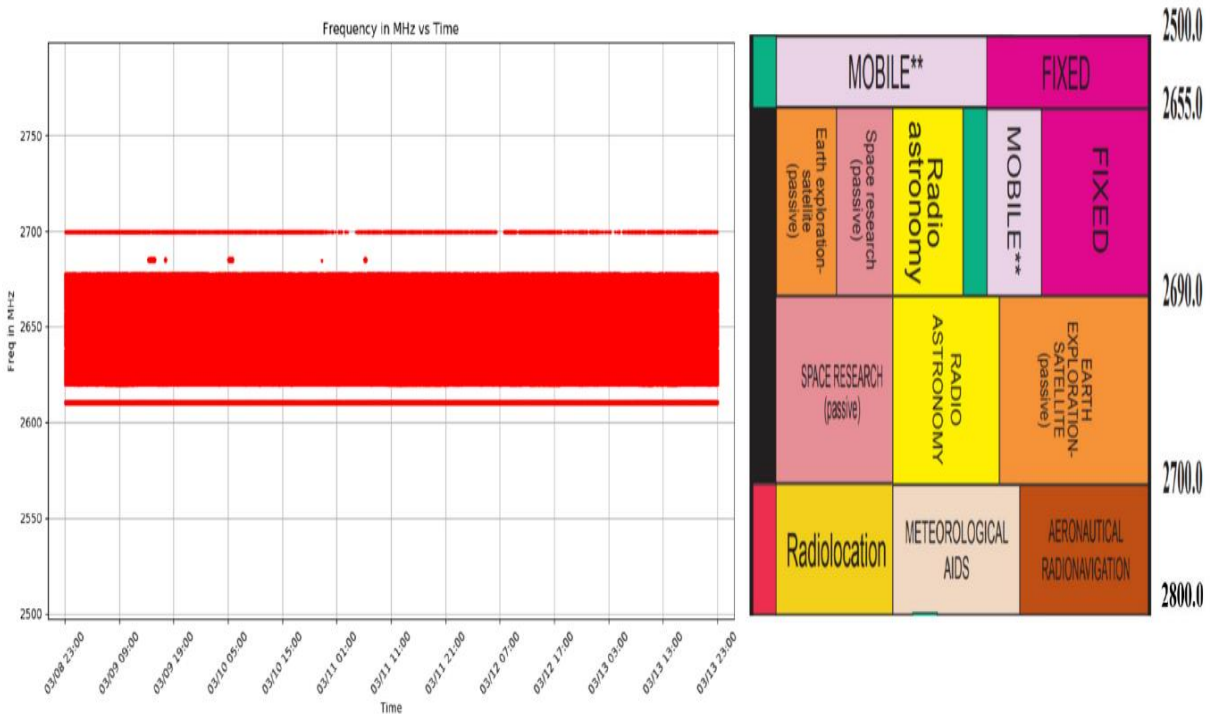

Figure 3.15 2500 MHz to 2800 MHz Spectrum Allocation and Usage

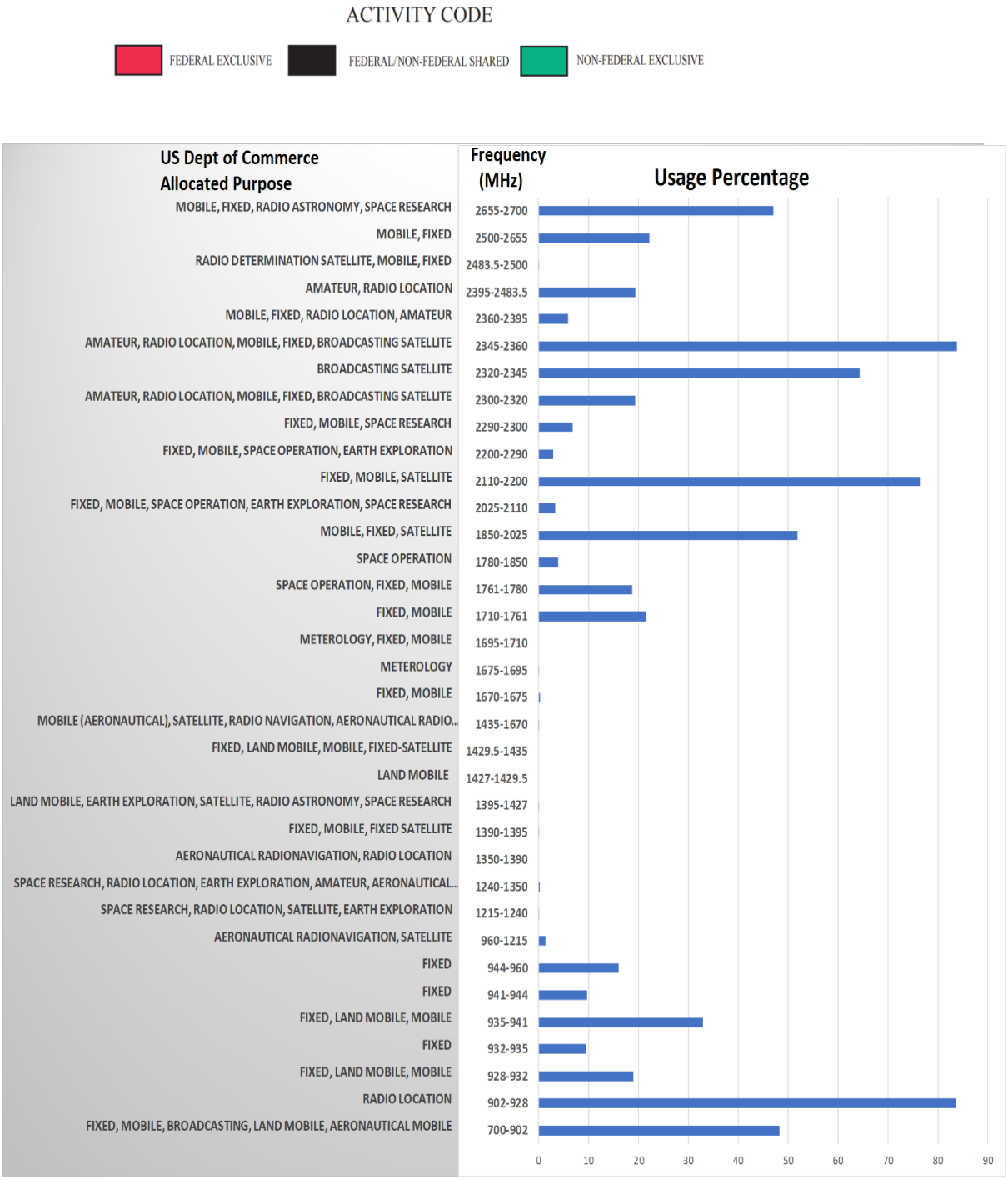

Figure 3.16 Spectrum allocation category and usage percentage

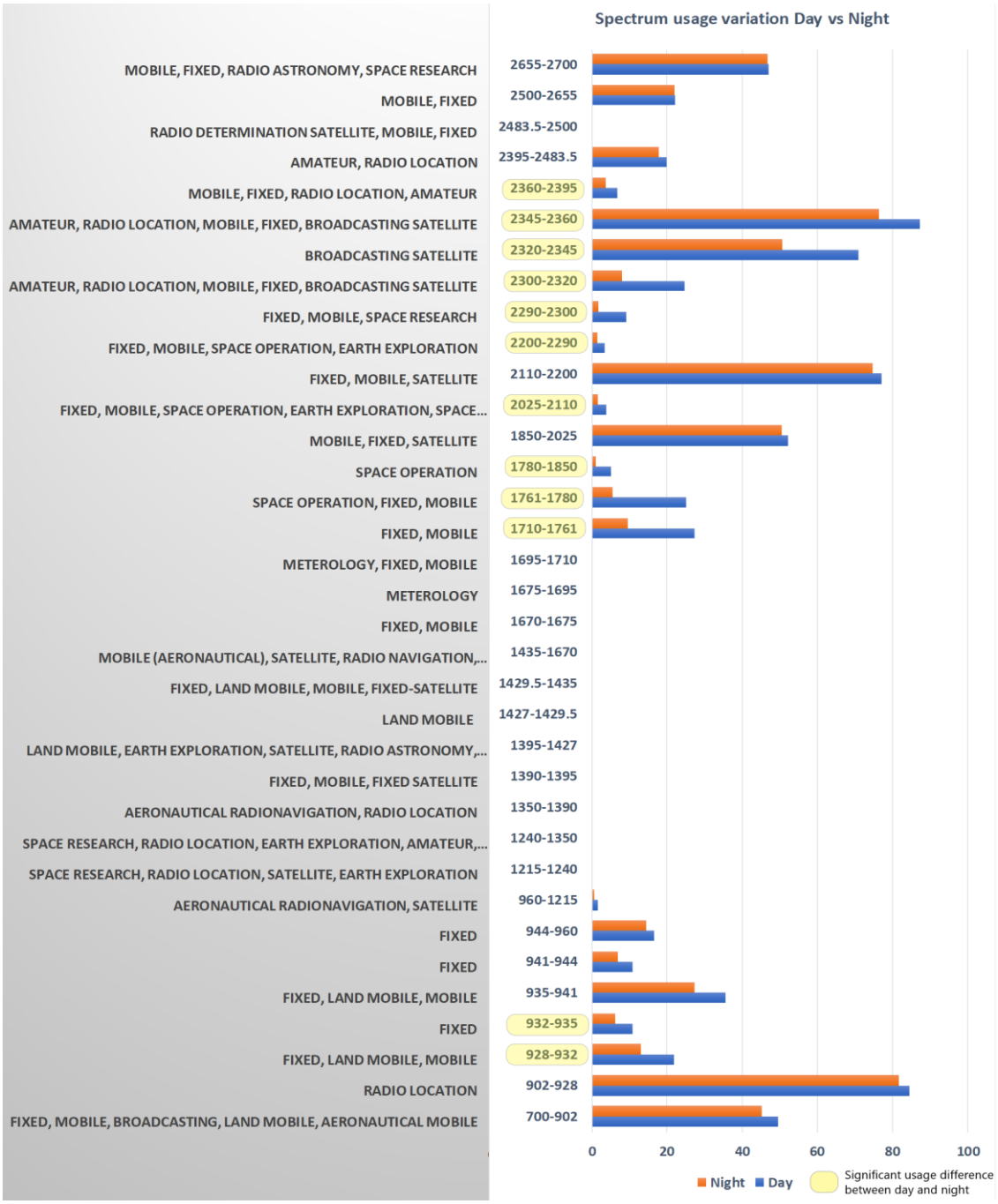

Figure 3.17 Spectrum usage difference between day and night

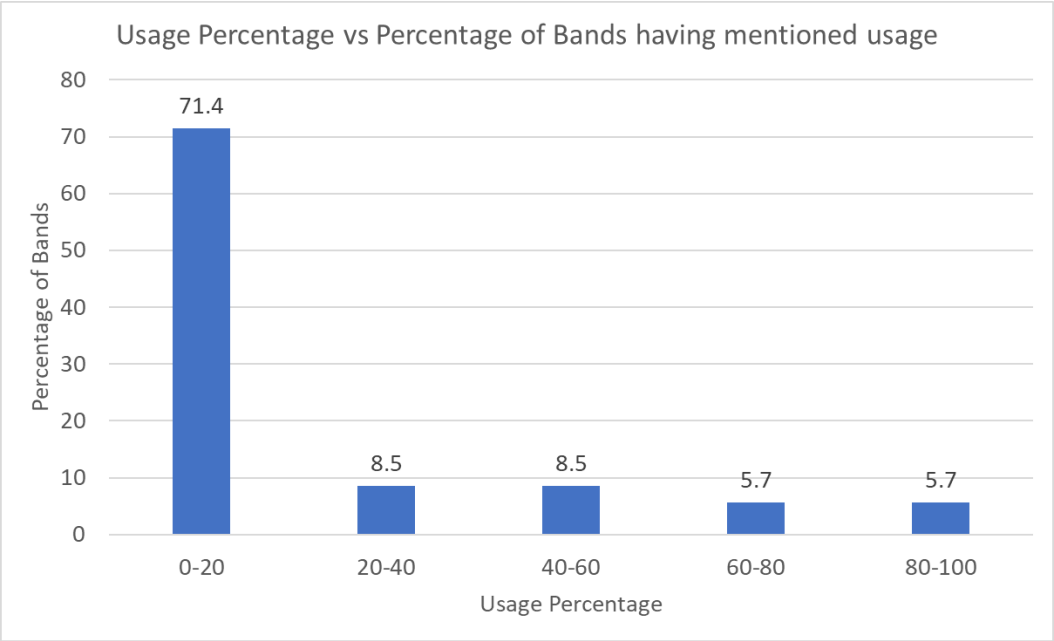

Figure 3.18 Usage percentage vs Percentage of Bands

Table 3.1 Range and duration of collected data

Frequency Range	700 MHz to 2.8 GHz
Collection Period	March 8th, 2020 11:00 PM to March 13th, 2020

Table 3.2 NUC Specifications

Processor	Intel Core i7-8559U
Memory	32 GB
Storage	250 GB NVMe

CHAPTER 4

SPECTRUM PREDICTION

Spectrum prediction allows predicting the power of a channel and, in turn, the occupancy state of the channel for future time slots. It provides three key advantages as stated below:

- Conserves time and energy spent on spectrum sensing
- Gives an insight into the best frequency to be used
- Shows the state of the frequency bands for a large number of future slots

Without spectrum prediction, an opportunistic user (OU) needs to perform spectrum sensing for a large set of frequencies and determine the presence of a signal in each of them before actually using the frequency to transmit. Spectrum prediction also allows OU to select the best channel that has the highest potential to be available when predicted by different mechanisms.

We consider a wireless communication system where transmissions are performed in well-defined time slots as in a time-division multiplexed system. The OU needs to perform spectrum sensing and spectrum decision in each time slot before the transmission. Our motivation for spectrum prediction is based on the presence of temporal variations in the spectrum usage, as shown in Section 3.

As a part of this work, we develop a spectrum prediction framework with different Long Short-Term Memory (LSTM) architectures in deep learning and present extensive experiment results with real-world spectrum data that we collect.

Deep learning has proven to be a very valuable tool in various fields, including image processing and natural language processing. Applying deep learning methods for spectrum prediction remains an active research area with the potential for significant improvements [10]. Complex LSTM models in deep learning with multi-layered networks have the ability to perform well on time-series prediction [21, 22].

LSTM is an artificial recurrent neural network architecture that can learn long-term dependencies. An LSTM unit is composed of a cell, an input gate, an output gate, and a forget gate. The cell remembers values over arbitrary time intervals, and the three gates regulate the flow of information into and out of the cell [11].

We explore and validate the following Long Short-Term Memory (LSTM) architectures for spectrum time-series prediction.

1. Multi-step Univariate stacked LSTM
2. Single-step Multivariate stacked LSTM
3. Multi-step Encoder-Decoder LSTM
4. Multi-step Multivariate stacked LSTM

4.1 Multi-step Univariate stacked LSTM (MSUL)

LSTM networks can learn to forecast long sequences in one shot. We leverage this to predict multi-step spectrum power values of a selected frequency, i.e., given the historical

power observations at the time, (t-1, t-2, ..., t-k), the model predicts power values for time, (t, t+1, …, t+m) using only the power values as the input feature.

4.1.1 Supervised Data Creation

Our dataset is structured as shown in Figure 4.1. In our example dataset creation, five data points for predictions are shown with both input and forecast window size selected as 5. The values in the slots, (t1, t2, …, t5) of the first spectrum prediction point represent the power values in the shown timeslot. The corresponding label of the data point is represented by the values in the slots (t6, t7, …, t10). The power values are received over time, so the dataset is created by sliding a window with a fixed length, L. The power values are normalized to values between 0 and 1. This normalization makes the training and convergence faster and also helps in learning the problem effectively. The results we present in this document are obtained using the input window size of 30 and the forecast window size set to 100.

4.1.2 Univariate Stacked LSTM Network

As illustrated in Figure 4.2, our first model is based on a univariate unidirectional stacked LSTM architecture consisting of two hidden layers and one dense layer with 100 hidden states in every layer. We use the learning rate of 0.001, RELU activation function, and mean squared error as the loss function.

For our experiments, we create the dataset by moving the window one step at a time. In this example, as shown in Fig. 4.2, the input contains power value for a frequency for 9-timesteps (t0 to t8). As we have set the input step size or input window size as 3, the

raw input data is reshaped into four samples. We use 50% of the collected data for training, 20% for validation, and the remaining 30% for testing.

Each reshaped sample contains the input data for 3-time steps. In the training phase, we feed the next 3-time steps' data as the label. Our LSTM model requires input in a three-dimensional format. In this example, our values for three dimensions are given in Table 4.1.

4.2 Single-step Multivariate stacked LSTM Network (SSML)

Neural Networks, like LSTM networks, can model problems with multiple input features. This is a great benefit in time-series forecasting over classical linear forecasting methods as it is very difficult to adapt to multivariate input forecasting problems in classical methods. We predict a single future power value for each of the input frequencies. This prediction can help the opportunistic user gain insight on which frequencies can be reliably predicted by the multi-step forecast models.

4.2.1 Supervised Data Creation

The dataset is constructed through a sliding window, as shown in Figure 4.3. Suppose the length of the sliding window is 3; the label for the training is the power value of all the channels of time slot t4, and the model outputs the predictive power values of corresponding channels for the same time slot t4. The window is forwarded one timestep ahead to form the next datapoint. We create the whole dataset for the network using this sliding window approach.

4.2.2 Stacked LSTM Network

The structure of the LSTM network constructed in this case has five hidden layers, all of which are comprised of LSTM layers. The first layer has 300; the second layer 200 hidden; the third layer 100, the fourth layer 70, and the fifth layer, has 50 hidden units. Each layer has RELU as the activation function, and the output of one layer is fed as the input to the next layer. The output of the last hidden layer goes into a Dense layer. We use Mean Square Error as the loss function, and the Adam optimizer is used for updating network weights. With input frequencies from f1, f2, …, fN, N input features are used, and the model predicts one power value corresponding to each of the N input frequencies.

4.3 Multi-step Encoder-Decoder LSTM

The Encoder-Decoder LSTM is a special type of Recurrent Neural Network designed to solve sequence-to-sequence (seq2seq) problems. Given the multiple time steps as the input and multiple time steps as the output, this type of problem is referred to as many-to-many sequence prediction problem. The Encoder-Decoder LSTM is proven to be very effective in seq2seq prediction problems.

4.3.1 Supervised Data Creation

The dataset here is also constructed using a method similar to the one described in Section 4.1.1. Given the historical power observations at the time (t-1, t-2, ..., t-k) for a particular frequency, the model predicts power values for time (t, t+1, …, t+m) using only the power values as the input feature. However, the label, in this case, has three

dimensions - samples, timesteps, and features, unlike the previous case that had only two dimensions. The sliding window mechanism is used to create the entire dataset.

4.3.2 Encoder-Decoder LSTM Network

This architecture comprises of two models – the encoder model and the decoder model. The encoder model is used for reading the input sequence and encode it into a fixed-length vector and this fixed-length vector is then fed into the decoder model that outputs the predicted sequence. Let t1, t2, …, t4 be the input sequence that is fed into the encoder LSTMs and t5, t6, …, t7 be the predicted sequence from the decoder LSTM. The decoder model here makes a one-step prediction for each element in the output sequence. This is a subtle difference from the previously seen stacked LSTM architecture in Section 4.1, as in practice, both approaches predict an output sequence of power values.

4.4 Multi-step Multivariate Stacked LSTM (MSML)

So far, we have seen Multi-step spectrum prediction with only a single input power variable or feature. Real-world spectrum prediction becomes more challenging when we need to include more than one feature and yet be able to predict power/occupancy across multiple time steps. This specific architecture of multi-step multivariate stacked LSTM has the ability to handle multiple input variables and be able to predict power values for more than one timestep.

4.4.1 Supervised Data Creation

We use the features of power and time to evaluate this architecture. Time, however, is cyclical in nature, i.e., hour 23 and hour 0 are close to each other than hour 0 and hour 3. So, we transform the time data in such a way that this cyclical property is preserved. This time feature is transformed into two new features, x, and y where (x,y) represents a coordinate of a unit circle. We compute the x and y components using the sine and cosine trigonometric functions. Figure 4.5 shows an example unit circle for the *hours* variable where x is the cosine component, and y is the sine component. Midnight (0) is on the right, and the hour increases counterclockwise. In this way, the hour 23 is very close to hour 0. The transformations (x,y) in our experiments are performed using equations 7 and 8.

$$x = cos\,(2\pi(\Delta s/S)) \quad (8)$$

$$y = sin\,(2\pi(\Delta s/S)) \quad (7)$$

where, Δs represents the seconds since midnight, and S represents the total number of seconds in a day.

We follow the sliding window approach to create the entire dataset. Every data point has three features power, cosine transformed, and sine transformed components. The sliding window approach is shown in Figure 4.6. In Figure 4.6, 3 timesteps are used to predict the next two time steps. t4 and t5 are predicted in the first data point represented by the red dotted box. Similarly, t5, t6, and t6, t7 are predicted in the second and third data points.

4.4.2 Multivariate Stacked LSTM Network

The structure of the LSTM network constructed in this case has three hidden layers, which are all comprised of LSTM layers. Each layer has 100 hidden units and RELU as the activation function, and the output of one layer is fed as the input to the next layer. The output of the last hidden layer goes into a Dense layer. We use Mean Absolute Error as the loss function, and the Adam optimizer is used for updating network weights. The model is trained for a particular frequency to predict power values of 100 timesteps with three input features.

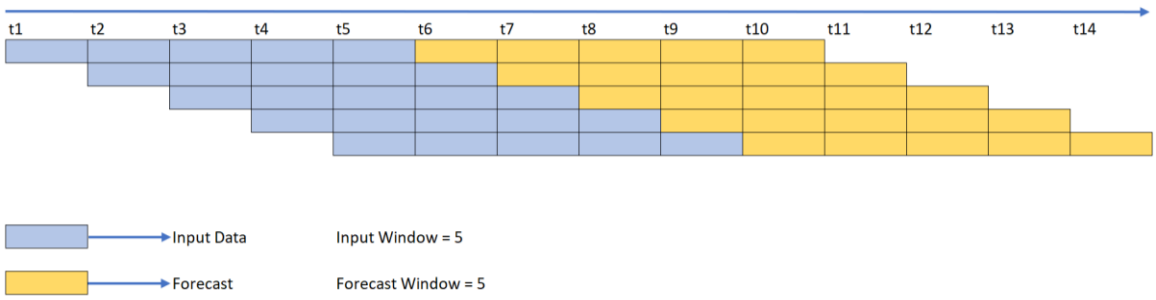

Figure 4.1 Dataset Figure

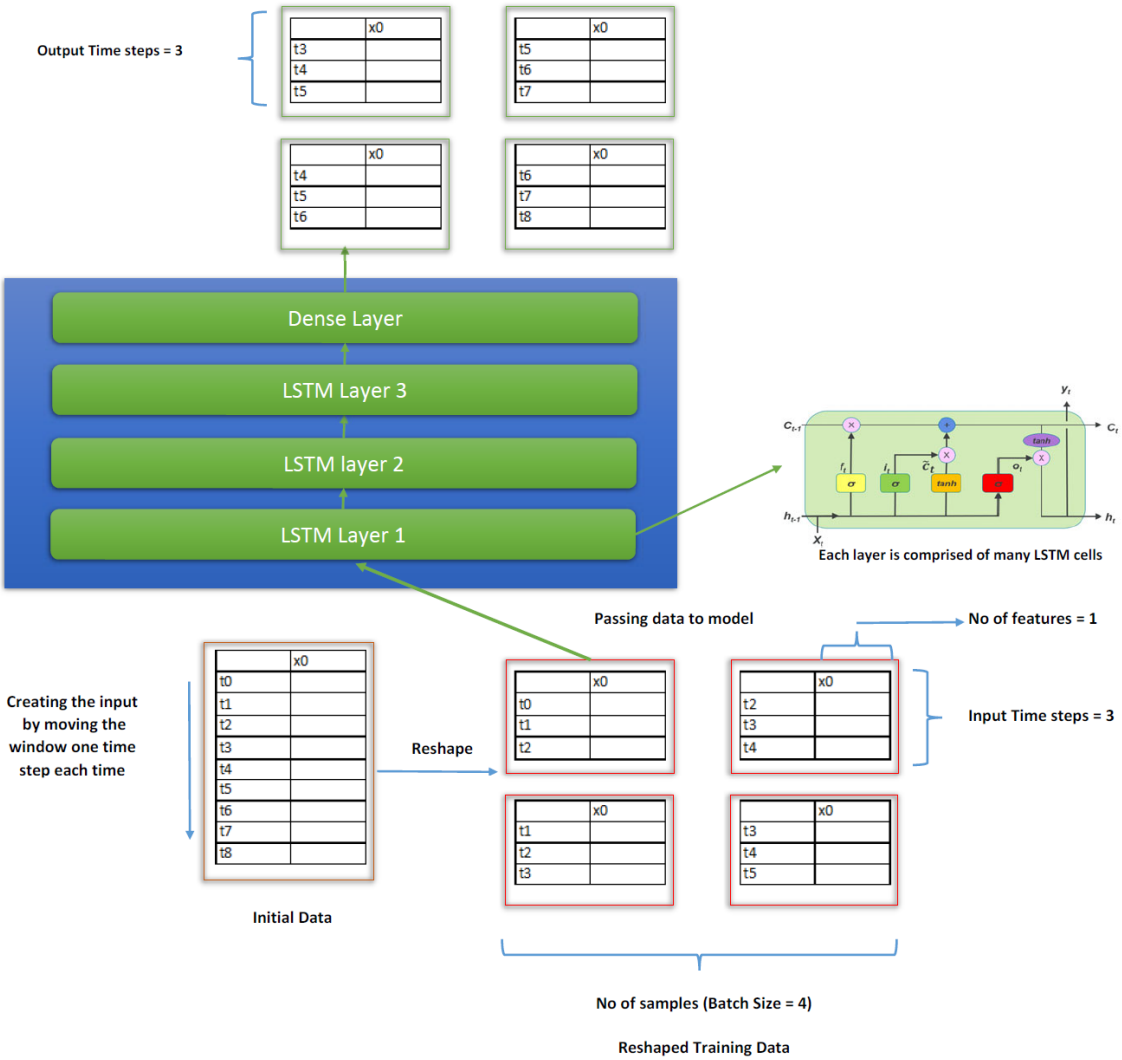

Figure 4.2 Univariate Stacked LSTM Architecture

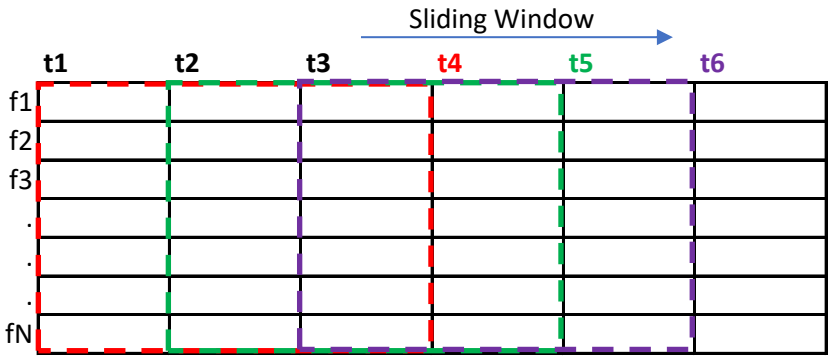

Figure 4.3 Dataset for Single-step Multivariate LSTM

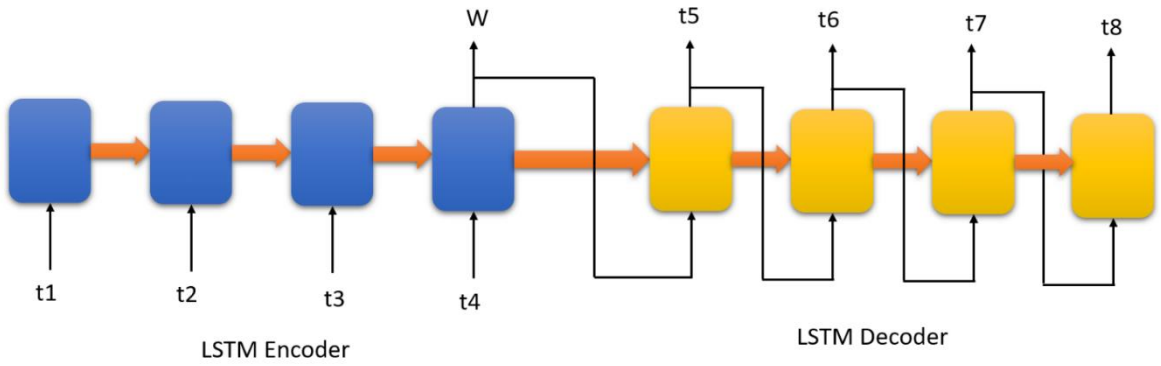

Figure 4.4 Encoder-Decoder LSTM

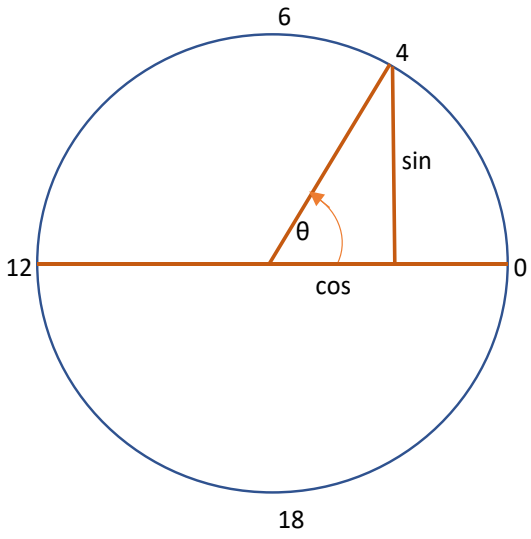

Figure 4.5 Time unit circle

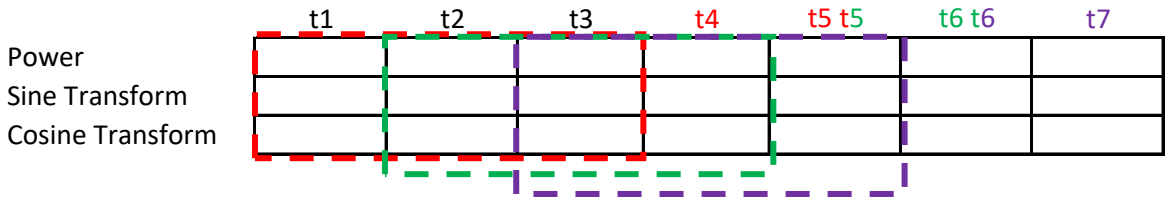

Figure 4.6 Data creation for multi-step multivariate LSTM

Table 4.1 LSTM Input Dimensions

Dimensions	**Example**	**Experiment**
Number of Features	1	1
Input Time Steps	3	10
Batch Size	4	10

CHAPTER 5

EVALUATION

We evaluate the performance of all the models based on a walk-forward validation. The test data is provided to the model by progressing one timestep each time. Thus, the model is always fed with the latest k lag observations, where k is the input window size.

5.1 Evaluation Metrics

We use the metric 1 below to evaluate the real-valued output of the models. The remaining metrics are used to evaluate the performance of the binary occupancy output:

1. Root Mean Square Error (RMSE)
2. Accuracy
3. F-score
4. False Positives, False Negatives
5. True Positives, True Negatives

The RMSE (Root Mean Square Error) is used to validate the real number outputs from the model, as it imposes a severe penalty on large errors in prediction. In our evaluation, we have calculated RMSE as follows for each forecast window:

$$RMSE = \sqrt{\frac{\sum_{i=1}^{n}(Predicted_i - Observed_i)^2}{n}}$$

We also convert the predicted power values to binary occupancy states by applying an appropriate threshold. The binary values are then validated using precision, recall, and F-Score, as described in Figure 5.1.

5.2 Baselines

We also establish the baseline performance of the spectrum prediction problem. This baseline performance provides a point of comparison when evaluating the more sophisticated LSTM models. We use two types of baseline algorithms, one type for the regression part of the problem and the other for the classification part. The two baseline algorithms used are as follows:

1. Exponential Weighted Moving Average for Regression
2. Zero Rule Algorithm for Classification

5.2.1 Exponential Weighted Moving Average (EWMA)

The EWMA is used to predict the label of the spectrum power data corresponding to a frequency. EWMA for a spectrum power series, V_t is calculated recursively as follows:

$$V_0 = 0 \tag{9}$$

$$V_t = \beta V_{t-1} + (1-\beta)\theta_t \tag{10}$$

Here, β represents the degree of the decrease in the weight of older datum, a constant smoothing factor between 0 and 1. θ_t is the current power value and V_t is the value of the EWMA at the time, t.

Equation 10 shows that a single prediction can be made as the value of the prediction is dependent on the current true value. Also, the prediction is dependent on a single feature of power, so multiple variables cannot be incorporated to predict future power values. Therefore, to get a baseline for multi-step models, we use the same prediction value for all the predicted time steps.

5.2.2 Zero Rule Algorithm

In the Zero Rule Algorithm, we predict the most common class label in the training set. This means that if the majority of the label in the training set is label "1", this algorithm uses a single rule of predicting only label "1" for the testing set.

5.3 Evaluation of Frequency Bands using SSML

An opportunistic user needs to make the spectrum decision by selecting the best frequency channel for its application. The Single-Step Multivariate stacked LSTM (SSML) model can give insight about the best frequency band of width 150 KHz by associating an RMSE score with each frequency band. The OU can choose the best frequencies for its application by selecting frequency bands which are lower than a required RMSE score. The selected frequency channel can be evaluated for multi-step prediction by OU. Any choice of bandwidth can be used to evaluate the SSML models. We evaluate four different frequency bands with bandwidths of 5, 10, and 12 MHz. There

are, for example, 67 150KHz frequency bins in a 10MHz band. Figures 5.2 to 5.5 show the SSML model's performance for the four different bands. In all of these figures, the y-axis represents RMSE, and the x-axis represents the frequency values. These plots show how the future multivariate LSTM models are likely to perform for various frequencies, and this can guide OU to make the best choice in its spectrum decision phase. The red dot in the plots represents an example frequency, and it's the corresponding RMSE given by the model. We have highlighted one frequency from each of the range and its corresponding RMSE. We use these representative frequencies to further study other models.

5.4 Frequency Selection for Evaluation of Multi-step models

Our goal is to select frequencies that exhibit different usage patterns so that we can study the robustness of the multi-step spectrum prediction models. The selection of the representative frequencies is guided by the visual inspection of the spectrum occupancy plots and the result of the SSML models. Our selected frequencies and their behavior are shown in Table 5.1.

The four selected frequencies only serve as a subset of applicable frequencies. The spectrum prediction is applicable and can be extended to any frequency. To be applied on a new frequency, the multi-step models need to be trained on the desired frequency's usage data. The usage pattern of selected frequencies is illustrated in Figures 5.6 to 5.9. Each data point is collected every 6 seconds approximately. The red dot in Figures 5.6 to 5.9 indicates the observed power value.

5.5 Evaluation of Multi-Step Models

In this section, we present our regression experiment results of the three Multi-step LSTM models and the EWMA base model. All the multi-step models are based on 30 lag windows and a prediction length of 100 windows. Figure 5.10 illustrates the RMSE performance of 3 LSTM based models and the EWMA model across four representative frequencies. We compare the performance of all the LSTM models with that of EWMA in Figure 5.11. We see an improvement of almost 2% to 15%.

From Figure 5.10, we can observe that the 2357.925 MHz frequency band has the best forecast performance. It can be attributed to the fact that this band has regular high daytime usage and significantly low night-time usage, as shown in Figure 5.6. However, given that frequency 959.625 MHz does not have any particular usage pattern, the LSTM models perform significantly poorly when compared to other frequencies. Interestingly the LSTM models perform much better than EWMA. We also see in Figure 5.12 that the difference between the MSML and MSUL models is minor, with only about 2.3%.

5.6 Adaptive Threshold Mechanism

To estimate the occupancy state of the spectrum, we convert the predicted power values to binary occupancy state using a power threshold. For our dataset, we observe that the LSTM's predicted power values are very smooth. The predictions do not scale to the highs and lows present in the data, but the cycles and seasonality present in the data are forecasted correctly. The scaling issue poses a problem when we convert the power values to binary occupancy state using the original threshold. An example prediction of Frequency 704.125 MHz by stacked LSTM is shown in Figure 5.13.

We observe that with the correct threshold, the occupancy state can be determined effectively. We introduce an adaptive threshold mechanism that selects the best threshold by applying various thresholds in a predetermined range and selecting the one that provides the combined best F-Score and Accuracy across the forecast window.

The adaptive threshold selection shown in Figure 5.14 explores the space ranging from -90 to -73 for selecting the appropriate threshold. It then identifies the threshold value that maximizes both accuracies and F-scores across the entire forecast window. The original and selected adaptive thresholds are shown in Figure 5.15.

Figure 5.15 provides a comprehensive plot of both training and test data. The blue marker indicates the true data; an initial 50% of the data is used for training; the orange marker indicates the model's prediction on the training data. The next 20% data is used for validation, and the green marker indicates the LSTM's forecast on the validation data, and the red marker indicates the prediction on testing data.

We study in detail the impact of the adaptive threshold selection and determine that the adaptive threshold yields a better F-Score for both classes for different frequencies. For example, when applied to frequency 704.125 MHz, the Class 0 F-Score improves by 221.5%, and the Class 1 F-Score improves by 12%.

Figure 5.17 gives an insight into the accuracy of the models after the adaptive selected threshold is applied to the LSTM models. It also compares the accuracy of the LSTM models with that of the baseline majority model. We find that the LSTM models perform significantly better than the baseline majority model. Approximately, 96% accuracy is observed in the frequencies of 2357.925 for all the LSTM models. All the LSTM models are almost identical in performance except at 959.625 MHz.

As seen in the RMSE evaluation, prediction accuracy is also poor for 959.625 MHz, as no particular usage pattern is exhibited by this frequency. However, high prediction accuracy is seen in the bands that exhibit clear usage patterns.

		True Condition		Precision	Recall
	Spectrum Occupancy	Condition Occupied	Condition Idle		
Predicted Condition	Occupied	True Positive	False Positive	$\frac{\sum True\ Positive}{\sum Predicted\ Positive}$	$\frac{\sum True\ Positive}{\sum Condition\ Positive}$
	Idle	False Negative	True Negative	$\frac{\sum True\ Negative}{\sum Predicted\ Negative}$	$\frac{\sum True\ Negative}{\sum Condition\ Negative}$

F-Score (Class) =	$\frac{2.Precision\ .Recall}{Precision + Recall}$

Figure 5.1 Confusion Matrix Elements

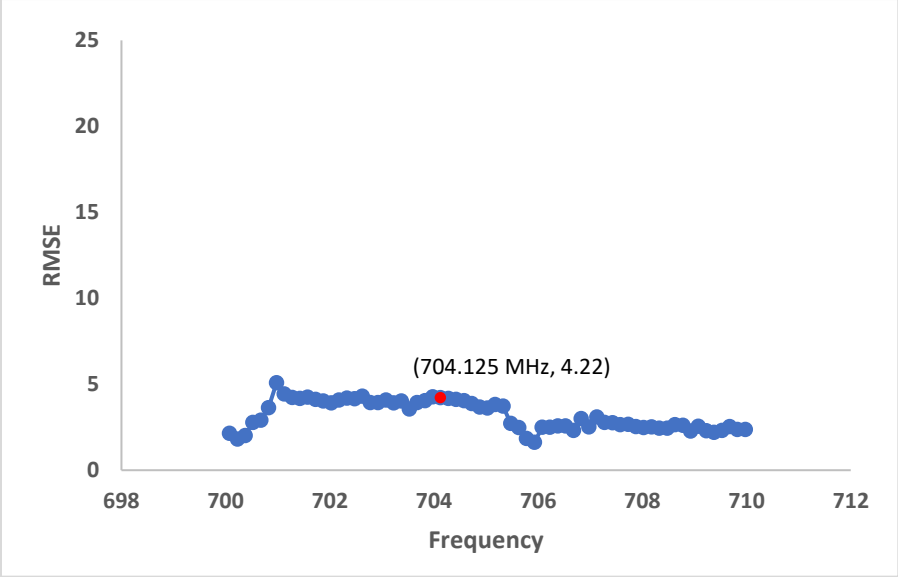

Figure 5.2 RMSE for the Frequency Band of 700 – 710 MHz

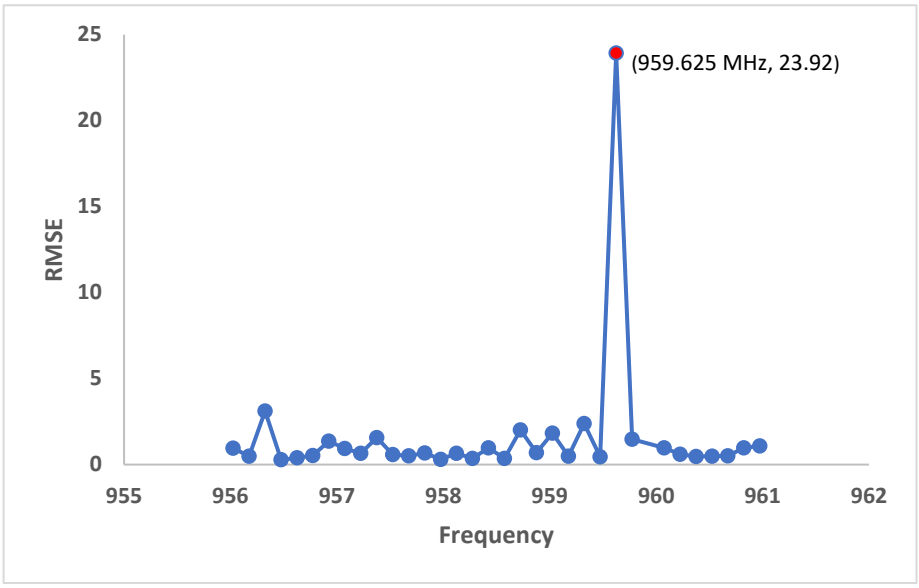

Figure 5.3 RMSE for the Frequency Band of 956 – 961 MHz

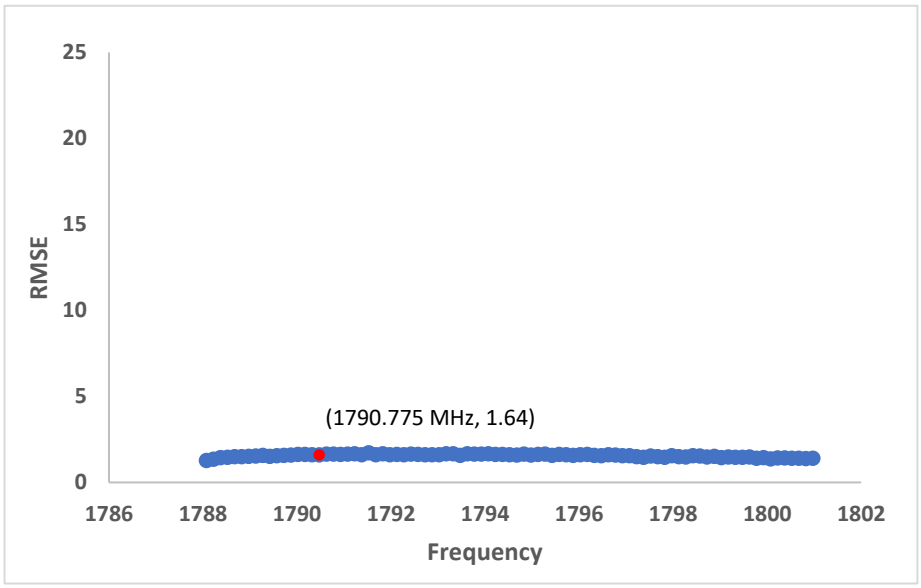

Figure 5.4 RMSE for the Frequency Band of 1788 – 1800 MHz

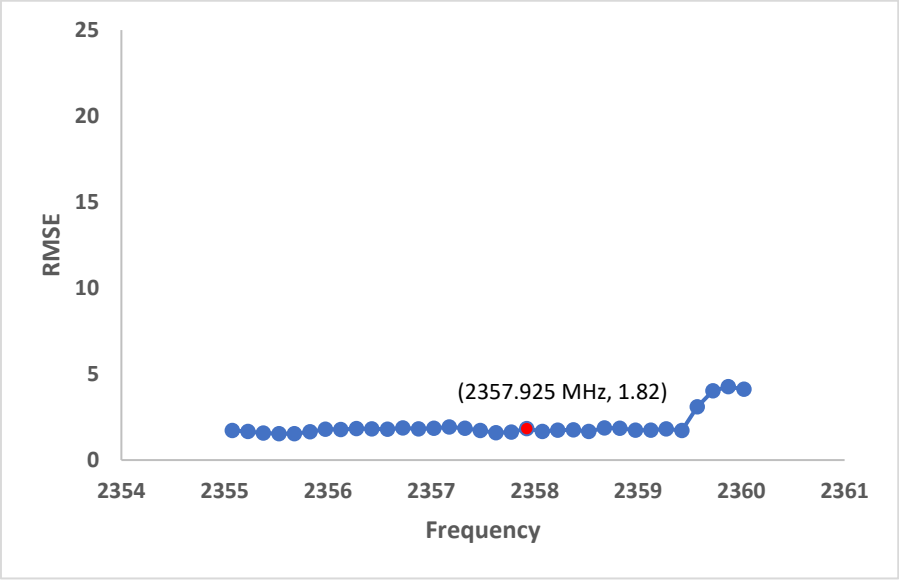

Figure 5.5 RMSE for the Frequency Band of 2355 – 2360 MHz

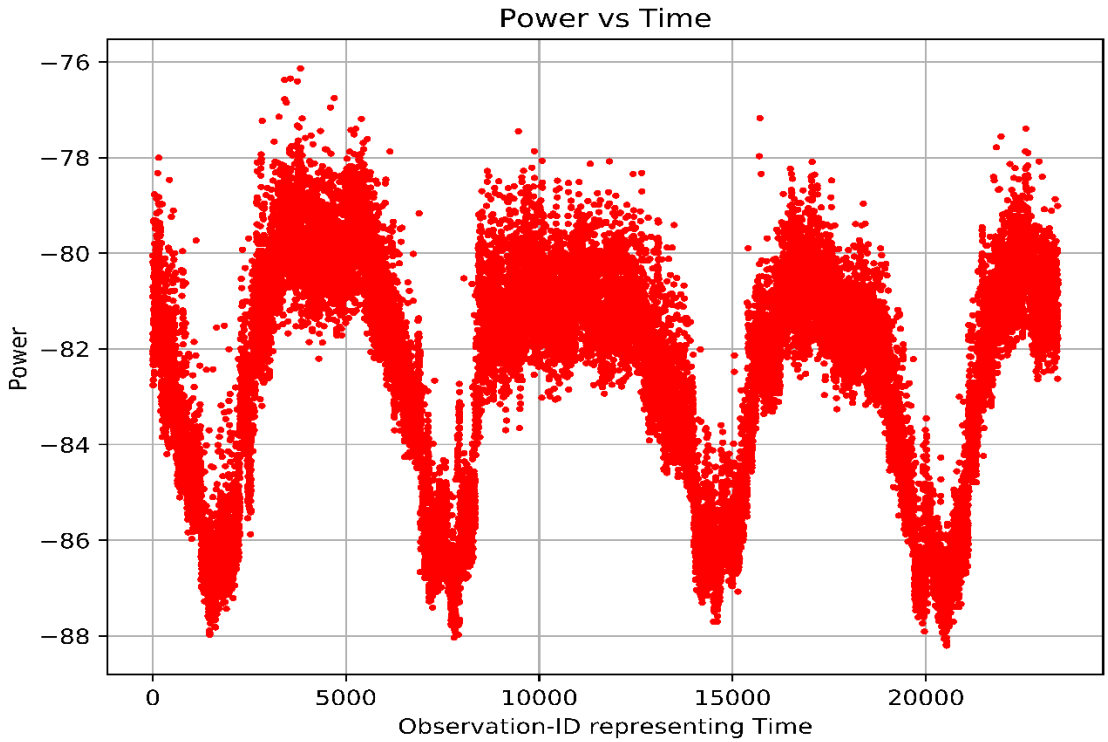

Figure 5.6 Usage pattern of 2357.925 MHz over four days

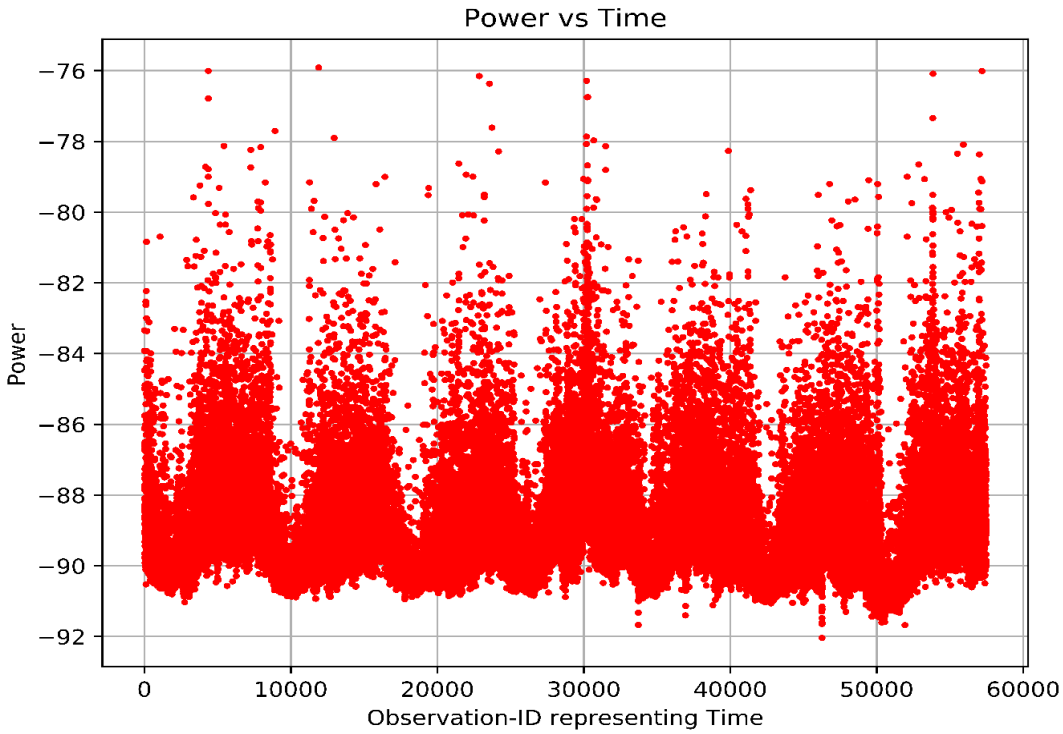

Figure 5.7 Usage pattern of 1790.775 MHz over seven days

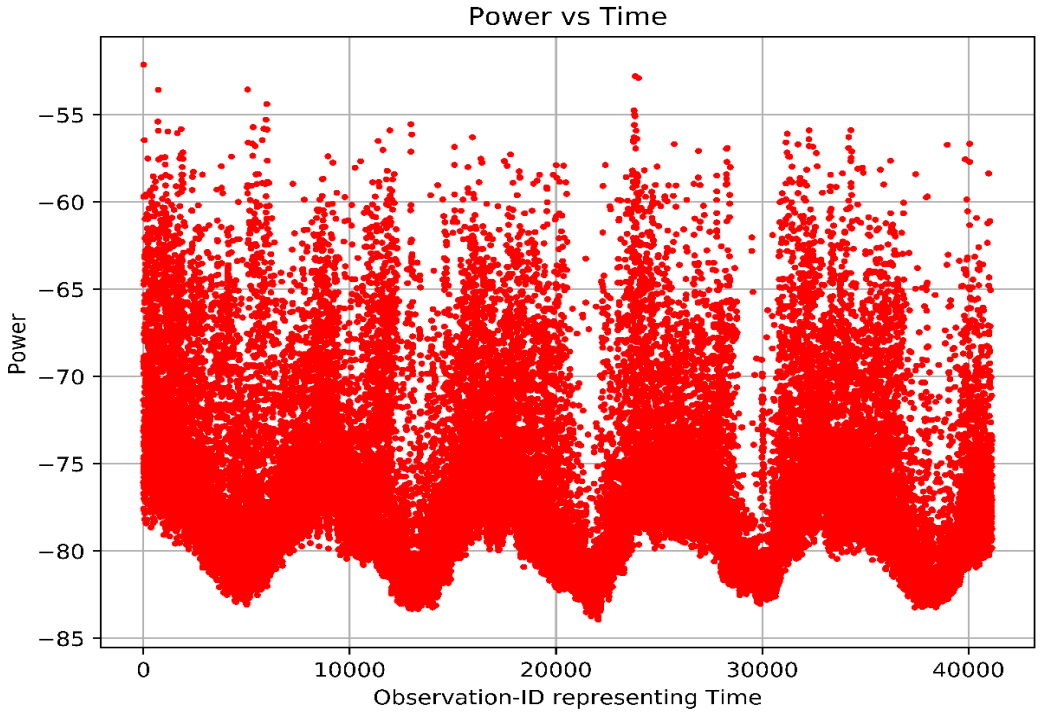

Figure 5.8 Usage pattern of 704.125 MHz over five days

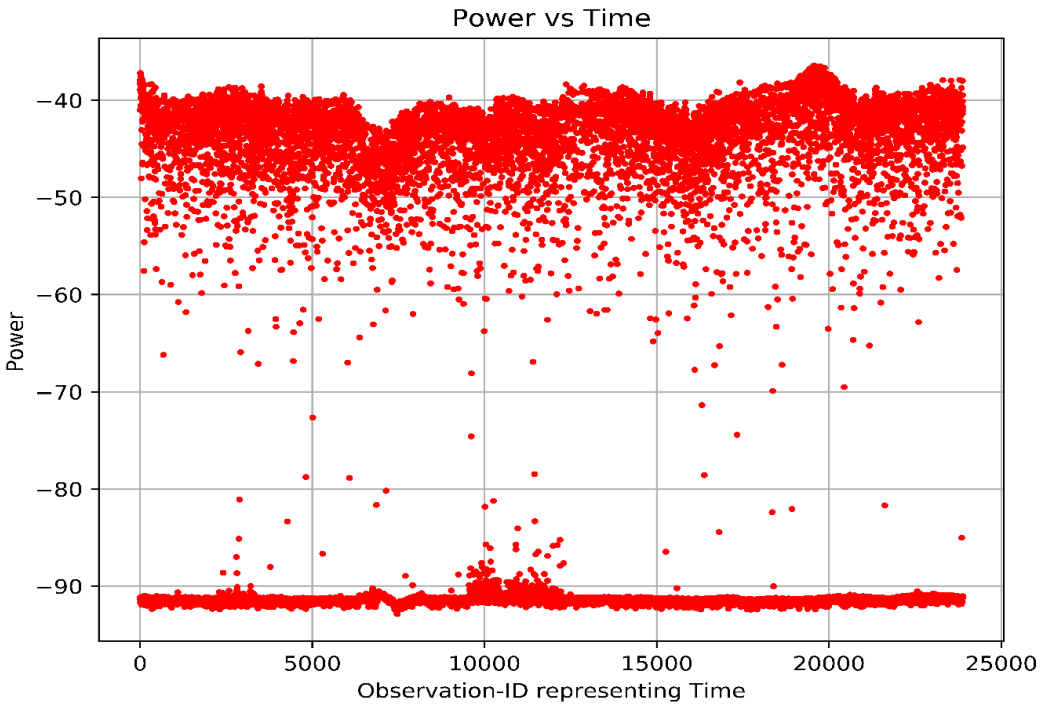

Figure 5.9 Usage pattern of 959.625 MHz over two days

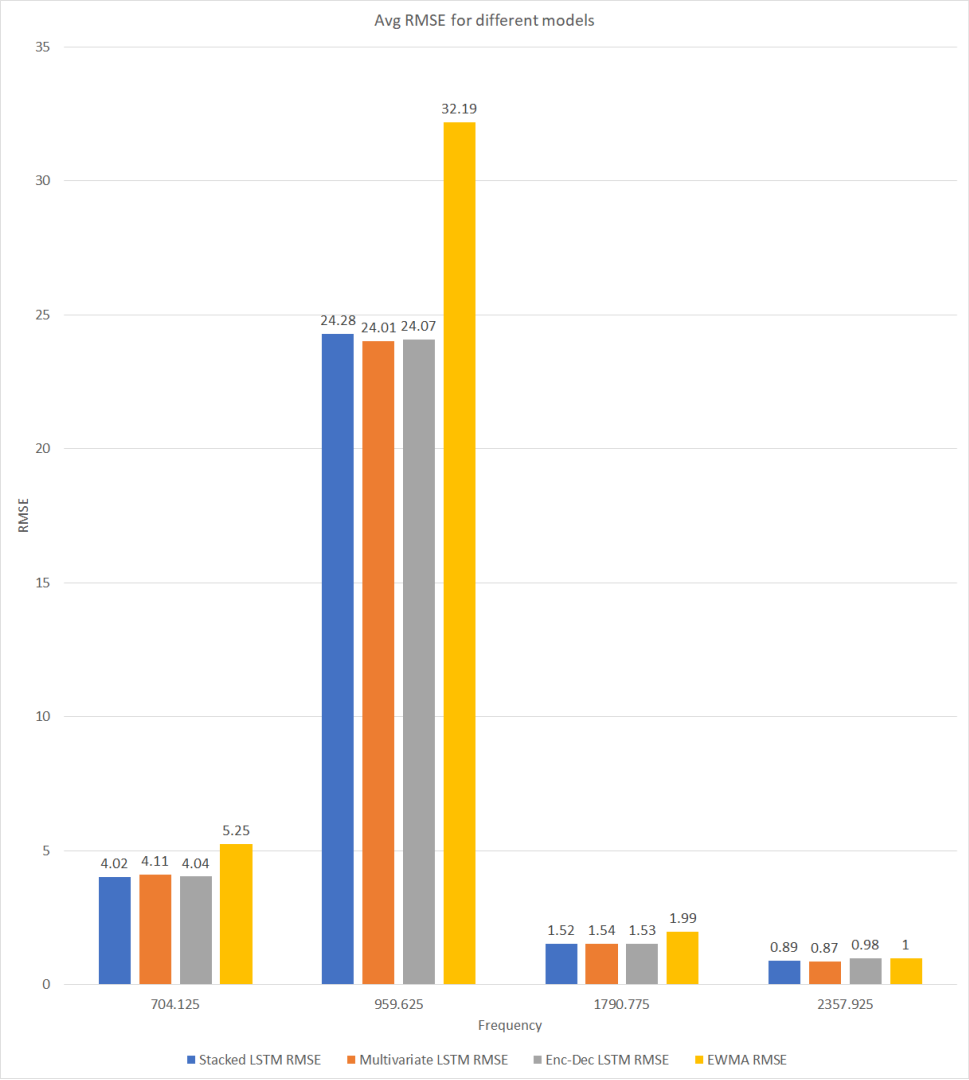

Figure 5.10 Average RMSE for 3 LSTM models and EWMA model

RMSE % Decrease in Comparison with EWMA			
Frequency	Stacked LSTM	Multivariate LSTM	Enc-Dec LSTM
704.125	11.94	9.49	11.39
959.625	9.02	10.25	9.97
1790.775	12.50	11.04	11.76
2357.925	12.36	14.94	2.04

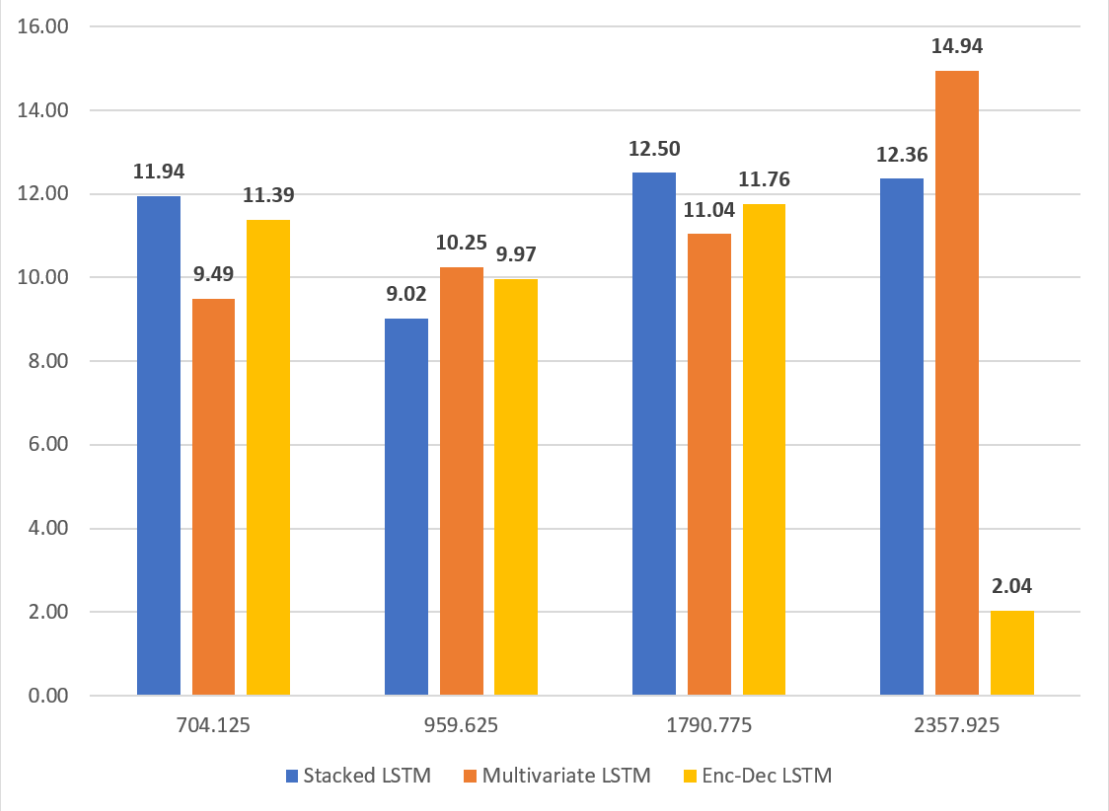

Figure 5.11 % increase in RMSE in EWMA compared to LSTM models

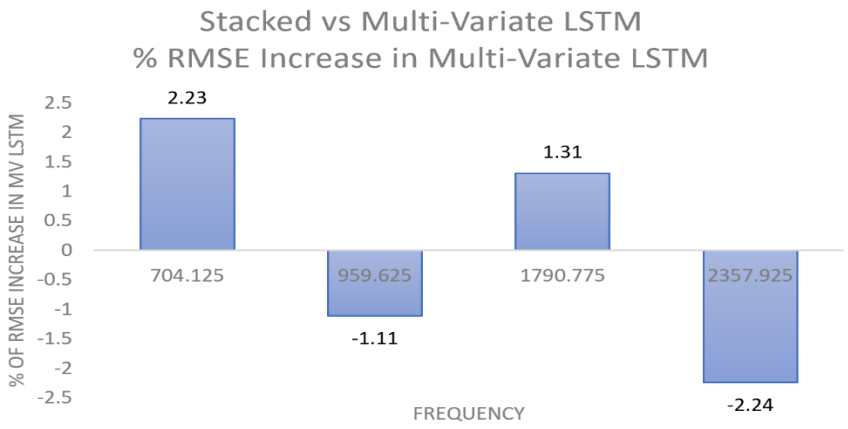

Figure 5.12 % increase in RMSE in MSML compared to MSUL

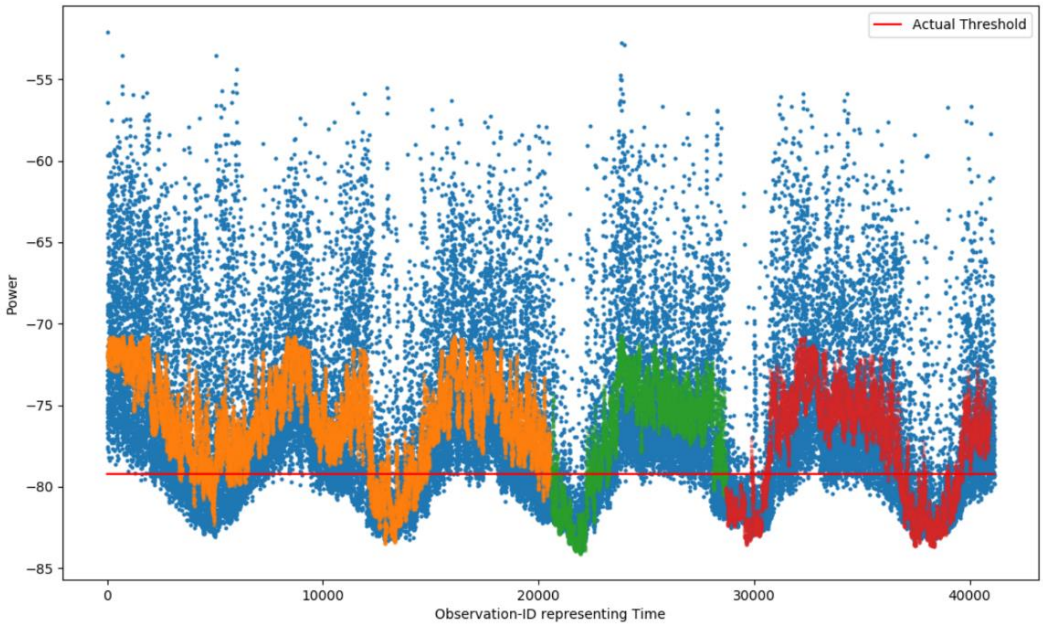

Figure 5.13 True power vs predicted power for Frequency 704.125 MHz

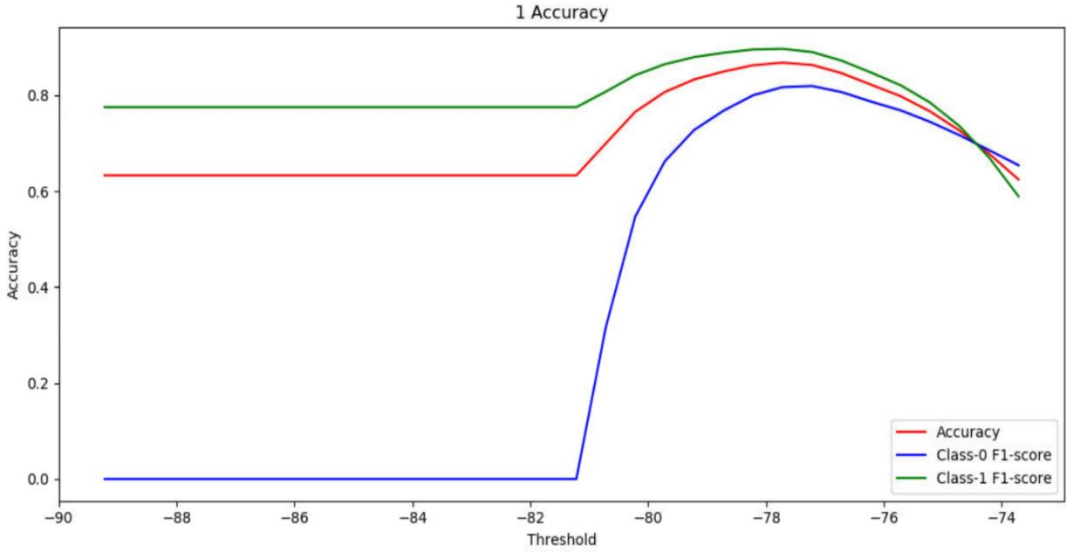

Figure 5.14 Adaptive Threshold Search

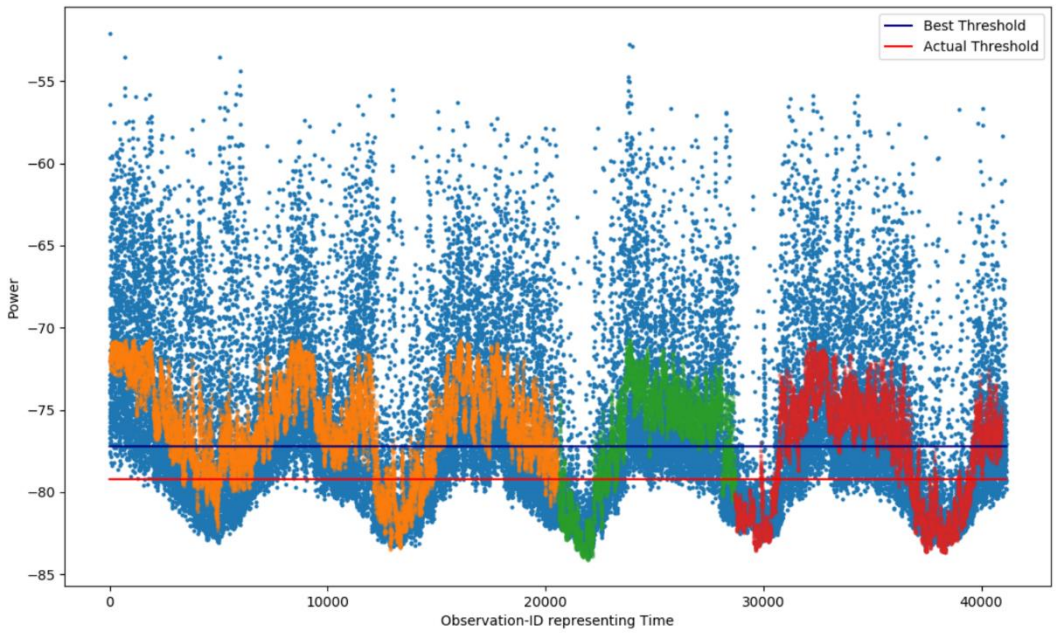

Figure 5.15 Adaptive Threshold Illustration

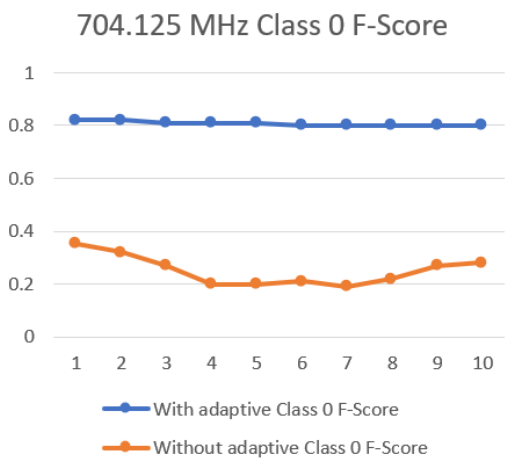

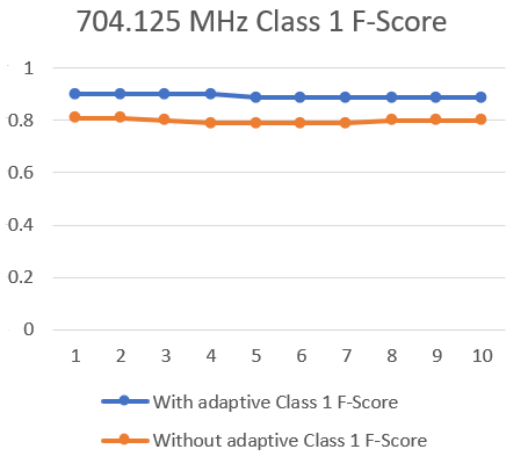

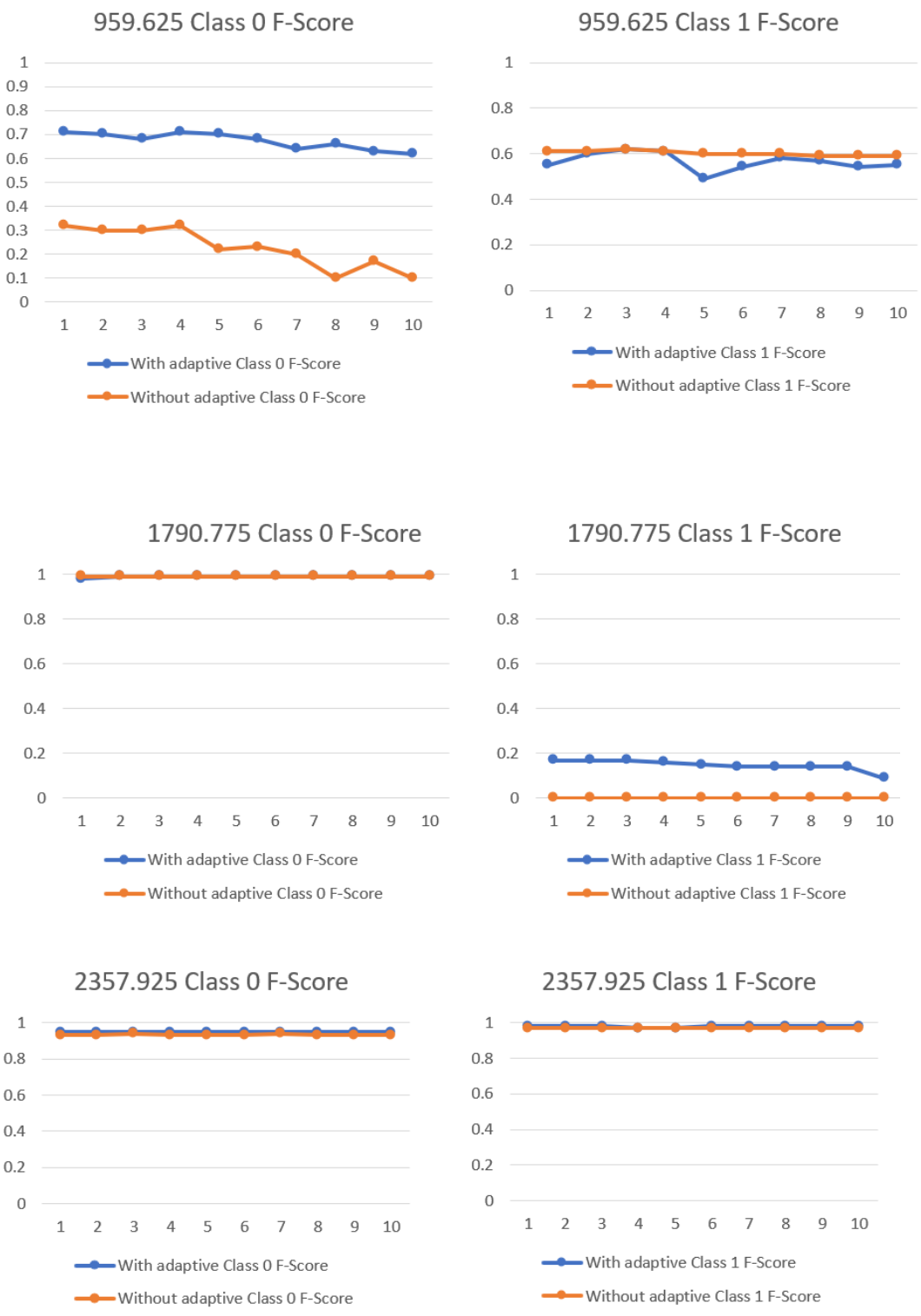

Figure 5.16 Comparison of F-Score with and without adaptive threshold

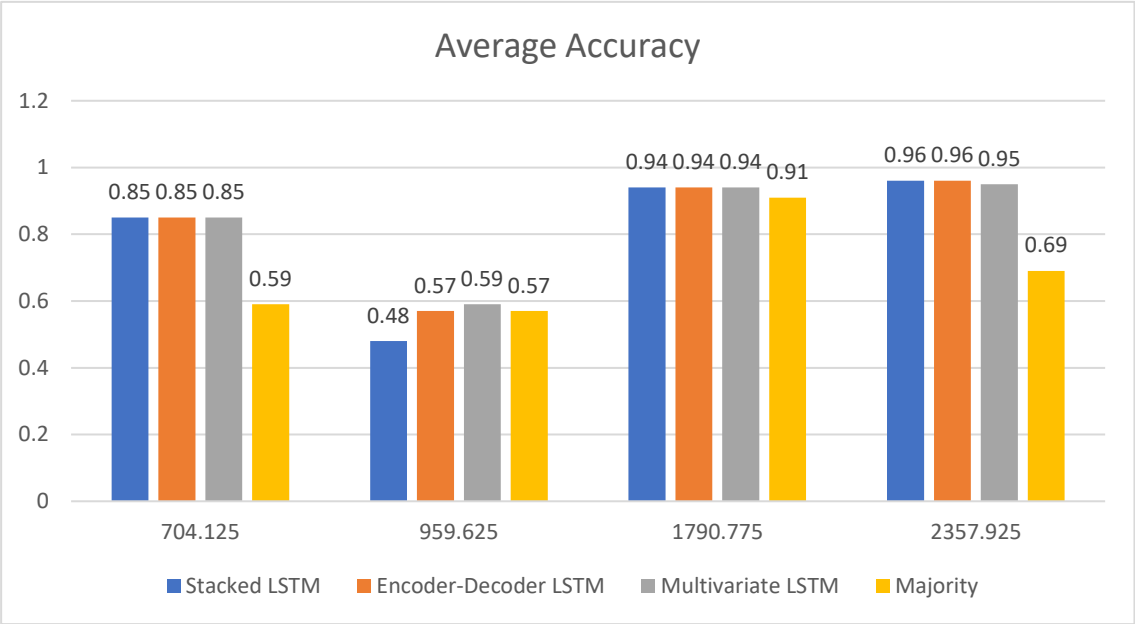

Figure 5.17 Accuracy of the models

Table 5.1 Selected frequencies and their usage pattern

Frequency	Usage Pattern
2357.925 MHz	Very high usage in the day and significantly low usage at night
1790.775 MHz 704.125 MHz	High usage in the day and relatively low usage at night
959.625 MHz	Exhibits no clear usage patterns

CHAPTER 6

FORECAST WINDOW LENGTH

6.1 Forecast Window Length Selection

While spectrum prediction has various advantages listed in the previous sections, the forecast window size remains a critical parameter for its applicability in real scenarios.

As stated in Table 6.1, a large forecast window increases the throughput by allowing an OU to access the channel continuously without having to pause transmission for determining the occupancy of the licensed user [20]. A large forecast window also reduces the overall energy spent by OU to sense and determine the occupancy state. However, when forecasting for larger windows using LSTM models, the error in the prediction increases with time. This phenomenon is displayed for Frequency 2357.925 MHz in Figure 6.1. This is also evident from the increasing rates False-Positives and False-Negative rates and a decreasing trend in Accuracy and F-scores when considering binary spectrum occupancy states.

Though the initial parts of the forecast window have the lowest RMSE, a small forecast window is not ideal as that involves sensing often. From our spectrum analysis, we observe that channels can have different usage patterns. Thus, each frequency may have a different forecast window that yields the best performance for that frequency.

6.2 LSTM based Window Selector

To solve the best window length for the OU, we introduce a new LSTM-based Window Selector, which predicts the best window length given a sequence of past power values. This selector takes the real-world power value of a frequency and the predicted values from an already trained MSUL model and then outputs a window-length. The components of the selector are illustrated in Figure 6.4.

30% of the spectrum data, which is the test data of the MSUL model, is used in the training and evaluation of this window selector system. The sliding window approach, described in Section 4.1.1, is used to create data points from the test data. The Window Selector (WS) Data Creation Module takes this created dataset as input, along with the predicted value from the MSUL model on the same dataset. It then labels each of the data points with a real number, which indicates the window length the MSUL model is able to predict correctly from the first prediction consecutively. This newly created dataset is then fed into the LSTM based WS model to train it.

6.2.1 LSTM based Window Selector Model

A 3-layer stacked LSTM architecture is used for this model with RELU as the activation function of each layer. The Adam optimizer for updating network weights and Mean Square Error as the loss functions are used for the training of the model. Early Stopper is used on the validation set to train the model for the optimal number of epochs. The training data consists of 50% of the total data, the next 20% data is kept for the validation set and the last 30% for testing the model. A new model needs to be trained and created for each individual frequency.

6.2.2 Window Selector Model Evaluation

We evaluate this model by choosing the window length of the past values to be 20. We choose the prediction window length to be 20 as well. This model can be extended to other past and prediction window lengths. The models' performance is summarized in Table 6.2, where RMSE is shown corresponding to each evaluated frequency.

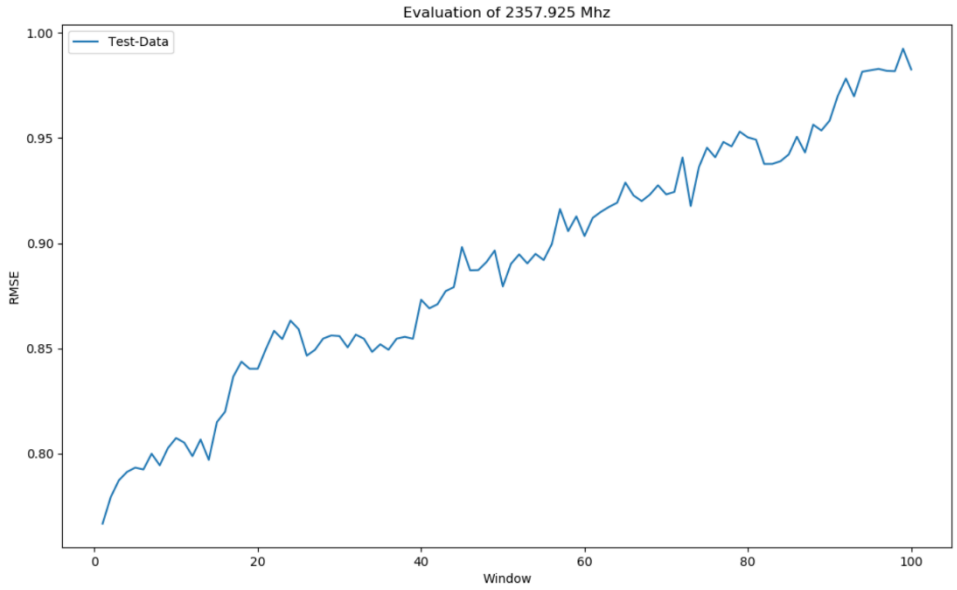

Figure 6.1 Increasing Trend in RMSE

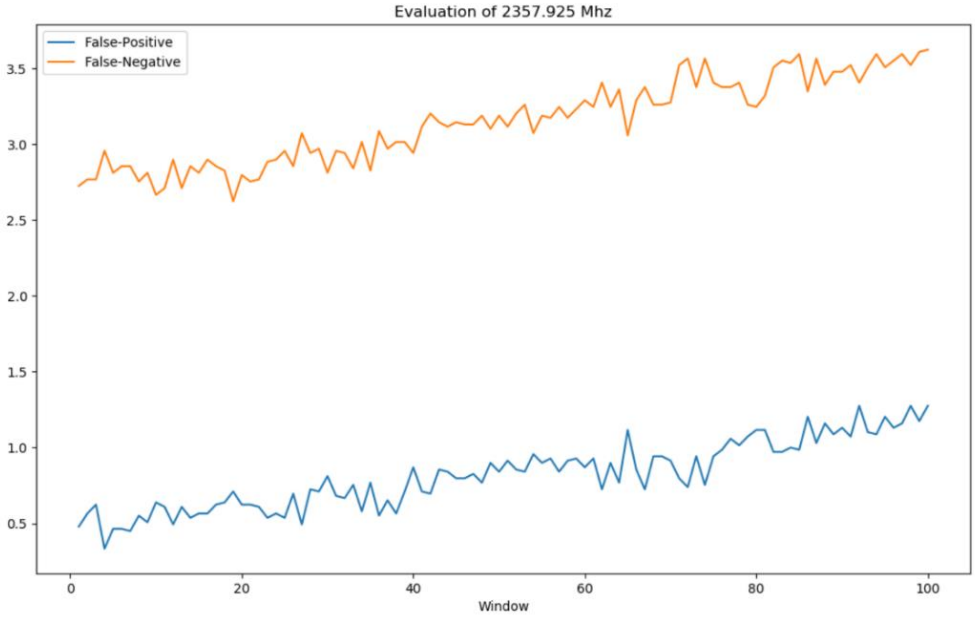

Figure 6.2 False Positive and False Negative over windows

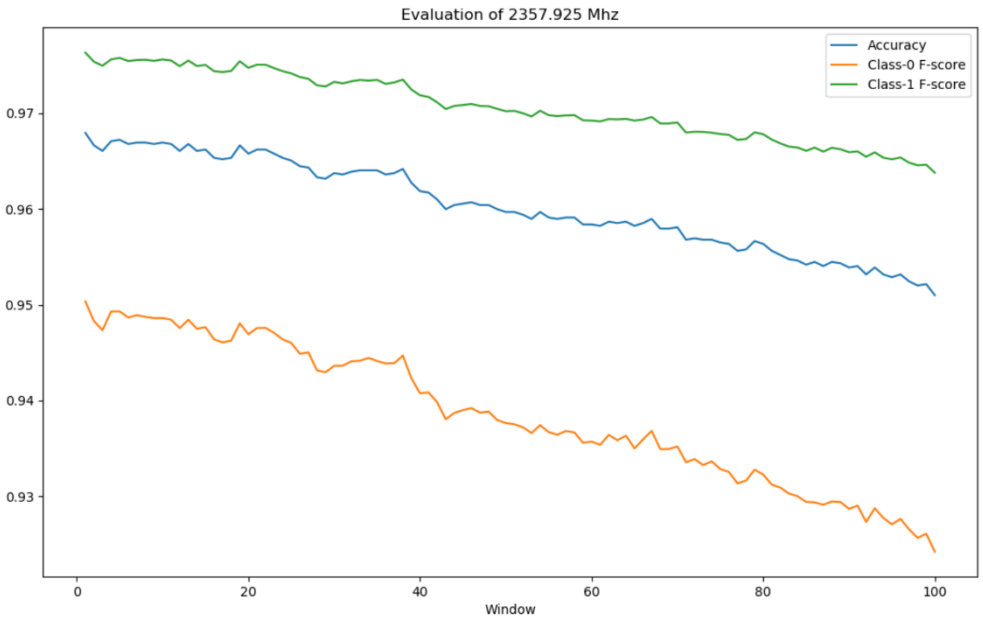

Figure 6.3 Accuracy and F-score over windows

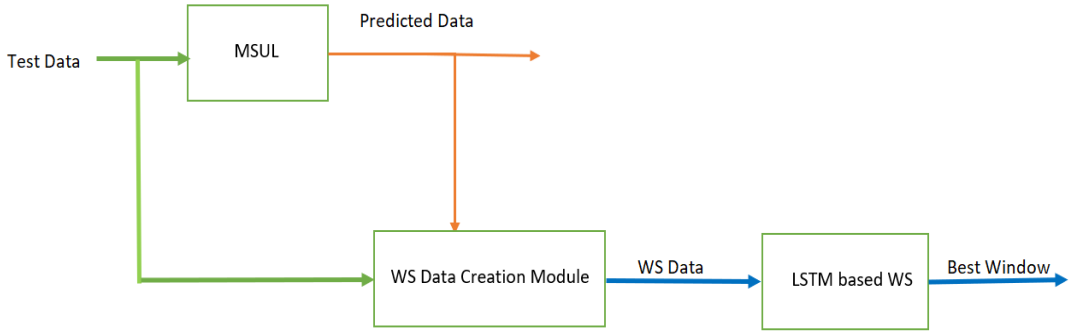

Figure 6.4 LSTM Based Window Selector

Table 6.1 Forecast window size pros and cons

Forecast Window	**Possible Pros**	**Possible Cons**
Large	Can increase throughput Can reduce energy spent on spectrum measurement	Can increase chances of False Negative thus leading to higher interference Can increase chances of False Positive thus leading to missed transmission opportunities
Small	It can reduce the chances of interference. It can reduce missed chances of transmission, i.e., identify available channels in a more timely fashion.	Can reduce throughput Can increase energy spent on spectrum measurement

Table 6.2 LSTM based Window Selector RMSE

Frequency	RMSE
704.125	6.8
959.625	1.97
1790.775	6.32
2357.925	4.55

CHAPTER 7

DISCUSSION

7.1 Spectrum Usage

We study spectrum usage of Salt Lake City, Utah, and find that the average spectrum usage of the frequencies in the range of 700-2800 MHz is only about 19%, and 70% of the frequency bands have usage of less than 20%. This study shows that there are bands that have the potential to be used for alternative services or systems. However, before using a band, especially the ones identified as less utilized for a new service, detailed contemporary studies need to be performed to understand the current status of the band. For the cases where the signals are not detected because of low power transmission, different threshold calculation mechanisms can be evaluated. In order to assess the variations of the spectrum usage, parallel measurements and surveys should be conducted on locations with different population densities, different geographic characteristics, and different user profiles. To assist such studies in the future with POWDER platform, we have developed plug-n-play tools which can be catered as per the need of the user. These tools can be customized to make measurements in the chosen frequency for a selected amount of time for any location. Our tools also have the capability to visualize spectrum usage at different granularities.

7.2 Spectrum Prediction

We use various LSTM based techniques, EWMA, and Majority prediction techniques for spectrum prediction. Single-step Multivariate stacked LSTM (SSML) can predict the spectrum power value of multiple frequencies in a single go, whereas EWMA based model can be used only for a single frequency at a time. For example, if one SSML model can predict future values for 100 frequencies at a time, 100 different EWMA models are needed to achieve the same purpose. EWMA model also can predict only one step in the future, unlike robust multi-step LSTM models, which can predict multiple steps in a one-shot. For our comparison, we assumed the same prediction for the entire forecast window in the case of EWMA. Furthermore, the EWMA model is dependent on all the past observations to predict future value. Hence these EWMA models cannot be deployed for opportunistic use as there would not be any available observation when the user is busy transmitting in the channel.

Our work gives an insight into how an opportunistic user can use the SSML model to evaluate various bands to narrow down the choices of the frequencies to be used for its transmission and then use multi-step LSTM models to forecast the availability of the channels corresponding to the selected frequency over multiple timeslots. LSTM based Window Selector model would then guide the user to use the best length of the forecast window. All these models can be trained and used for any choice of bands and bandwidth. Multi-step LSTM models can be trained and used to predict for any length of the forecast window. The hyperparameters of the models are optimized for the frequencies evaluated in this work. Multi-step models can work better on a different set of hyperparameters instead of the ones used in this work when applied to a different

frequency band. For data from a different location, training needs to be performed again before the models can be used. To avoid using the models which are trained on stale data, the models need to be retrained with newly collected data. This will help capture the deviations or changes from the original training data over time.

CHAPTER 8

CONCLUSION

We collected and analyzed spectrum usage data on the POWDER platform in Salt Lake City, Utah. We found that various segments of the spectrum remain underutilized. We also highlighted the segments of the spectrum where the usage pattern differs significantly between day and night.

Motivated by our spectrum usage findings, we explored LSTM models to perform spectrum prediction on four bands, each exhibiting a different usage pattern over time. We have explained in detail our choice of LSTM architectures and explained their performance in the selected frequencies. To overcome the challenges faced when converting the LSTM model's prediction to binary occupancy state, we introduced a new adaptive threshold parameter that significantly boosts the occupancy prediction performance. To minimize the chances of interference and maximize the throughput, we introduced a novel LSTM based Window Selector system. This system automatically outputs the best window length with the given power input data.

In the future, the performance for both single-step and multi-step predictions can be evaluated for other frequency bands to obtain a broader understanding of the correlation between the usage pattern of the spectrum and LSTM's performance. Window Selector model can be evaluated with multi-step models other than the MSUL model. Other types of deep learning techniques, such as Multilayer Perceptron (MLP) and Convolutional

Neural Networks (CNN), can be applied in the Window Selector model to find the best window.

References

[1] M. A. McHenry, P. A. Tenhula, D. McCloskey, D. A. Roberson and C. S. Hood, "Chicago spectrum occupancy measurements & analysis and a long-term studies proposal," in *Proceedings of the First International Workshop on Technology and Policy for Accessing Spectrum*, New York, NY, USA, 2006.

[2] F. H. Sanders, B. J. Ramsey and V. S. Lawrence, "Broadband Spectrum Survey at San Francisco, California, May-June," US Department of Commerce, National Telecommunications and Information, 1995.

[3] F. H. Sanders and V. S. Lawrence, "Broadband spectrum survey at Denver, Colorado," US Department of Commerce, National Telecommunications and Information, 1995.

[4] F. H. Sanders, "Broadband spectrum surveys in Denver, CO, San Diego, CA, and Los Angeles, CA: methodology, analysis, and comparative results," *1998 IEEE EMC Symposium. International Symposium on Electromagnetic Compatibility. Symposium Record (Cat. No. 98CH36253),* vol. 2, pp. 988-993, 1998.

[5] M. H. Islam, C. L. Koh, S. W. Oh, X. Qing, Y. Y. Lai, C. Wang, Y.-C. Liang, B. E. Toh, F. Chin, G. L. Tan and others, "Spectrum Survey in Singapore: Occupancy Measurements and Analyses," in *2008 3rd International Conference on Cognitive Radio Oriented Wireless Networks and Communications (CrownCom 2008)*, IEEE, 2008, pp. 1-7.

[6] Vienna, VA, USA, Tech. Rep. 20100323, "Shared spectrum company general survey of radio frequency bands (30 Hz to 3 GHz)," Vienna, VA, USA, 2009.

[7] J. Mitola, "Cognitive radio for flexible mobile multimedia communications," *Mobile Networks and Applications,* vol. 6, no. 5, pp. 435-441, 2001.

[8] X. Xing, T. Jing, Y. Huo, H. Li and X. Cheng, "Channel quality prediction based on Bayesian inference in cognitive radio networks," in *2013 Proceedings IEEE INFOCOM*, 2013.

[9] G. Ding, Y. Jiao, J. Wang, Y. Zou, Q. Wu, Y.-D. Yao and L. Hanzo, "Spectrum Inference in Cognitive Radio Networks: Algorithms and Applications," *IEEE Communications Surveys and Tutorials,* vol. 20, no. 1, pp. 150-182, 2018.

[10] L. Yu, J. Chen and G. Ding, "Spectrum prediction via long short term memory," in *2017 3rd IEEE International Conference on Computer and Communications (ICCC)*, 2017.

[11] S. Hochreiter and J. Schmidhuber, “Long short-term memory,” *Neural Computation,* vol. 9, no. 8, pp. 1735-1780, 1997.

[12] L. Yu, Q. Wang, Y. Guo and P. Li, “Spectrum availability prediction in cognitive aerospace communications: A deep learning perspective,” in *2017 Cognitive Communications for Aerospace Applications Workshop (CCAA)*, 2017.

[13] A. Orange, “calibration-data-binder,” [Online]. Available: https://gitlab.flux.utah.edu/alex_orange/calibration-data-binder. [Accessed 14 6 2020].

[14] L. Yu, J. Chen, G. Ding, Y. Tu, J. Yang and J. Sun, “Spectrum Prediction Based on Taguchi Method in Deep Learning With Long Short-Term Memory,” *IEEE Access,* vol. 6, pp. 45923-45933, 2018.

[15] “POWDER WIRELESS RESEARCH,” University of Utah, [Online]. Available: https://powderwireless.net/. [Accessed 02 06 2020].

[16] I. Akyildiz, W.-Y. Lee, M. Vuran and S. Mohanty, “A survey on spectrum management in cognitive radio networks,” *IEEE Communications Magazine,* vol. 46, no. 4, pp. 40-48, 2008.

[17] H. Nyquist, “Thermal Agitation of Electric Charge in Conductors,” *Physical Review D,* vol. 32, no. 1, pp. 110-113, 1928.

[18] J. B. Johnson, “Thermal Agitation of Electricity in Conductors,” *Physical Review,* vol. 32, no. 1, pp. 97-109, 1928.

[19] H. Urkowitz, “Energy detection of unknown deterministic signals,” *Proceedings of the IEEE,* vol. 55, no. 4, pp. 523-531, 1967.

[20] X. Xing, T. Jing, H. Li, Y. Huo, X. Cheng and T. Znati, “Optimal Spectrum Sensing Interval in Cognitive Radio Networks,” *IEEE Transactions on Parallel and Distributed Systems,* vol. 25, no. 9, pp. 2408-2417, 2014.

[21] A. Graves, A.-r. Mohamed and G. Hinton, “Speech recognition with deep recurrent neural networks,” in *2013 IEEE International Conference on Acoustics, Speech and Signal Processing*, 2013.

[22] M. Hermans and B. Schrauwen, “Training and Analysing Deep Recurrent Neural Networks,” in *Advances in Neural Information Processing Systems 26*, 2013.

[23] I. Sutskever, O. Vinyals and Q. V. Le, “Sequence to Sequence Learning with Neural Networks,” in *Advances in Neural Information Processing Systems 27*, 2014.